

# Gaia BP/RP spectra of stars in the XSL, UVES\_POP, NGSL, CALSPEC, and SPSS libraries.

M. Messineo<sup>1,2</sup>

<sup>1</sup>Dipartimento di Fisica e Astronomia, Universita' di Bologna, Via Gobetti 93/2, 40129, Bologna, Italy

<sup>2</sup>INAF-Osservatorio di Astrofisica e Scienza dello Spazio di Bologna, Via Gobetti 93/3, I-40129 Bologna, Italy

Received (reception date); Accepted (acceptation date)

## Abstract

Gaia DR3 matches for stars in the XSL, UVES\_POP, NGSL, CALSPEC, and SPSS libraries are checked. There are 447, 376, and 501 entries in the XSL, UVES\_POP, and NGSL libraries with Gaia DR3 IDs, and 292, 302, and 381 entries with Gaia DR3 BP/RP spectra, respectively. Available Gaia DR3 BP/RP spectra are retrieved and compared with the library spectra to perform an external verification of the absolute flux calibration of the Gaia BP/RP spectra.

**Key words:** stars: evolution — stars: supergiants — stars: massive

## 1 Introduction

Matches between Gaia DR3 and the spectral libraries XSL, UVES\_POP, NGSL, CALSPEC, and SPSS are here analysed. The X-shooter Spectral Library (XSL) (DR3) is described in Verro et al. (2022). The Recalibrated UVES-POP Library for Stellar Population Synthesis is presented by Borisov et al. (2022). The Next Generation Spectral Library (NGSL) is described in Pal et al. (2023). The spectrophotometric standard stars (SPSS) is a library of spectra specifically designed for the Gaia calibration, it includes  $\approx 150$  stars (Pancino et al. 2021). The CALSPEC library contains the STIS spectra that are flux standards on the HST system (Bohlin et al. 2019), CALSPEC link.

X0833); in other words these five entries are not included in the list of 830 published spectra (full table retrieved via Vizier).

A best-quality list of 449 spectra was also received from Verro et al. with 447 belonging to the table “xsl\_dr3\_xmatch\_GaiaEDR3\_xmatch\_GaiaDist\_KV\_2asec\_pure.csv”. The matches with `has_xp_continuous='true'` are 345. When considering the repeated XSL observations, the 345 matched corresponds to 292 stars.

The XSL spectra have a wavelength bin varying from 0.012 to 0.083 nm. The Gaia BP/RP spectral bin is 2 nm.

## 2 XSL and Gaia BP/RP

The work of Verro et al. (2022) delivers a list of 830 spectra, which are freely available on Vizier. A list with 807 matches (2arcsec radius) between the XSL spectra and Gaia DR3 data points was used `xsl_dr3_xmatch_GaiaEDR3_xmatch_GaiaDist_KV_2asec_pure.csv`.

The used table contains five entries for which no spectra are available in the tar file (X0008, X0227, X0429, X0457, and

### 2.1 Comparison and residuals plots

In the github webpage

<https://lamortadella.github.io/BPRPLibraries/index.html>, there is a display page with the original XSL spectra (cyan) and overlaid the Gaia BP/RP spectra (black). A rebinned version of the XSL spectra is created (red curve) to match the resolution and wavelength scale of the Gaia data – by integrating the XSL spectra within each Gaia wavelength bin.

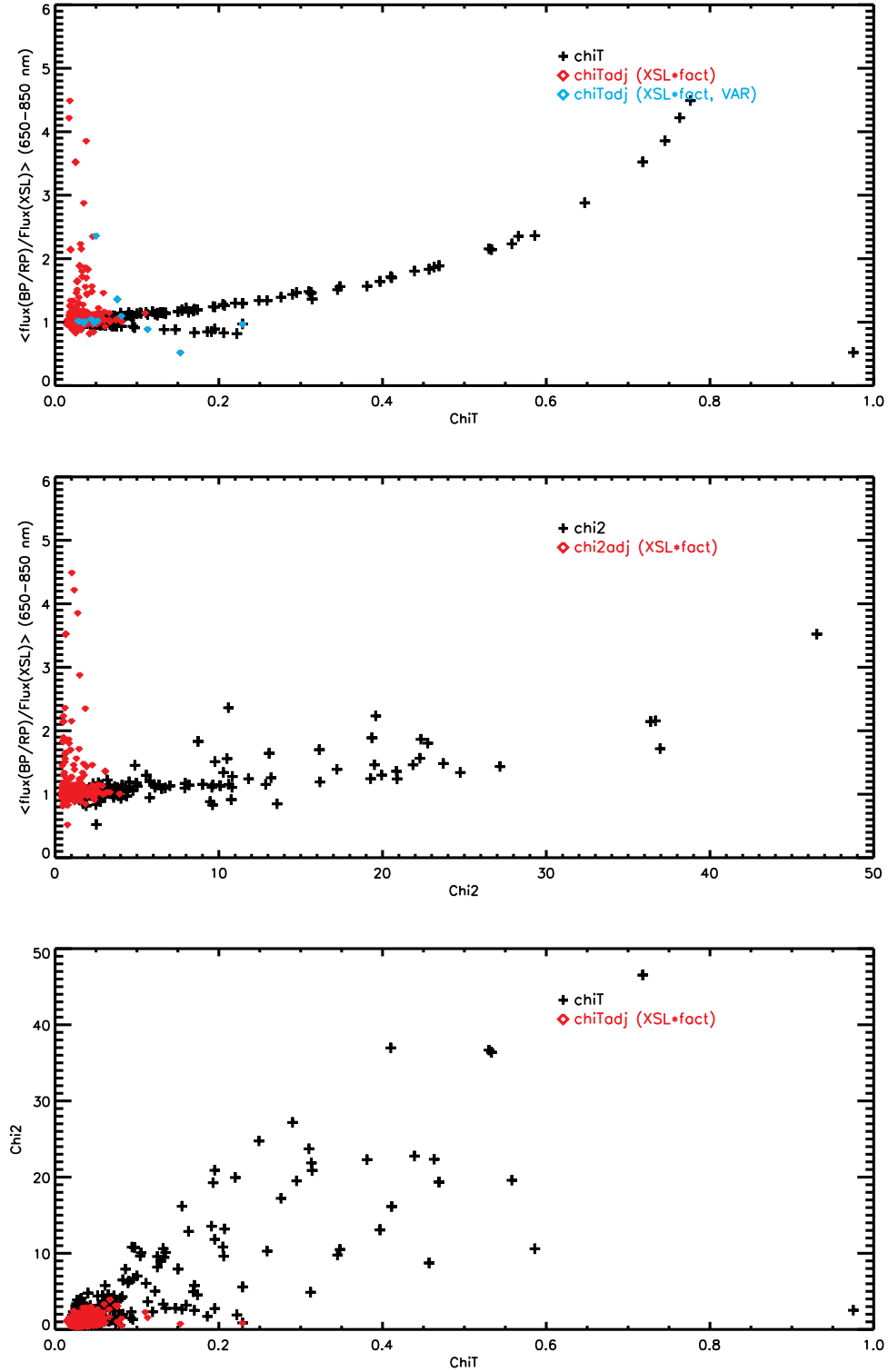


**Fig. 1.** *Upper panel:* XSL: the fact value, i.e., the average flux ratio between 700 and 750 nm (BP/RP-XSL) versus the  $\chi^2_{\text{IT}}$  values (black plus signs). A  $\chi^2_{\text{ITadj}}$  value is the  $\chi^2_{\text{IT}}$  of the modified spectrum  $\text{XSL} \times \text{fact}$ . The  $\chi^2_{\text{ITadj}}$  are much smaller than the  $\chi^2_{\text{IT}}$  values. The slopes of the XSL spectra do require a correction. The  $\chi^2_{\text{IT}}$ , here, is merely a measure of the percentage of deviations between the two vectors. *Middle panel:* XSL: the fact value, i.e., the average flux ratio between 700 and 750 nm (BP/RP-XSL) versus the  $\chi^2_2$  values (black plus signs). A  $\chi^2_{2\text{adj}}$  value is the  $\chi^2_2$  of the modified spectrum  $\text{XSL} \times \text{fact}$ . *Lower panel:* XSL: the  $\chi^2_{\text{IT}}$  versus the  $\chi^2_2$  values (black plus signs).

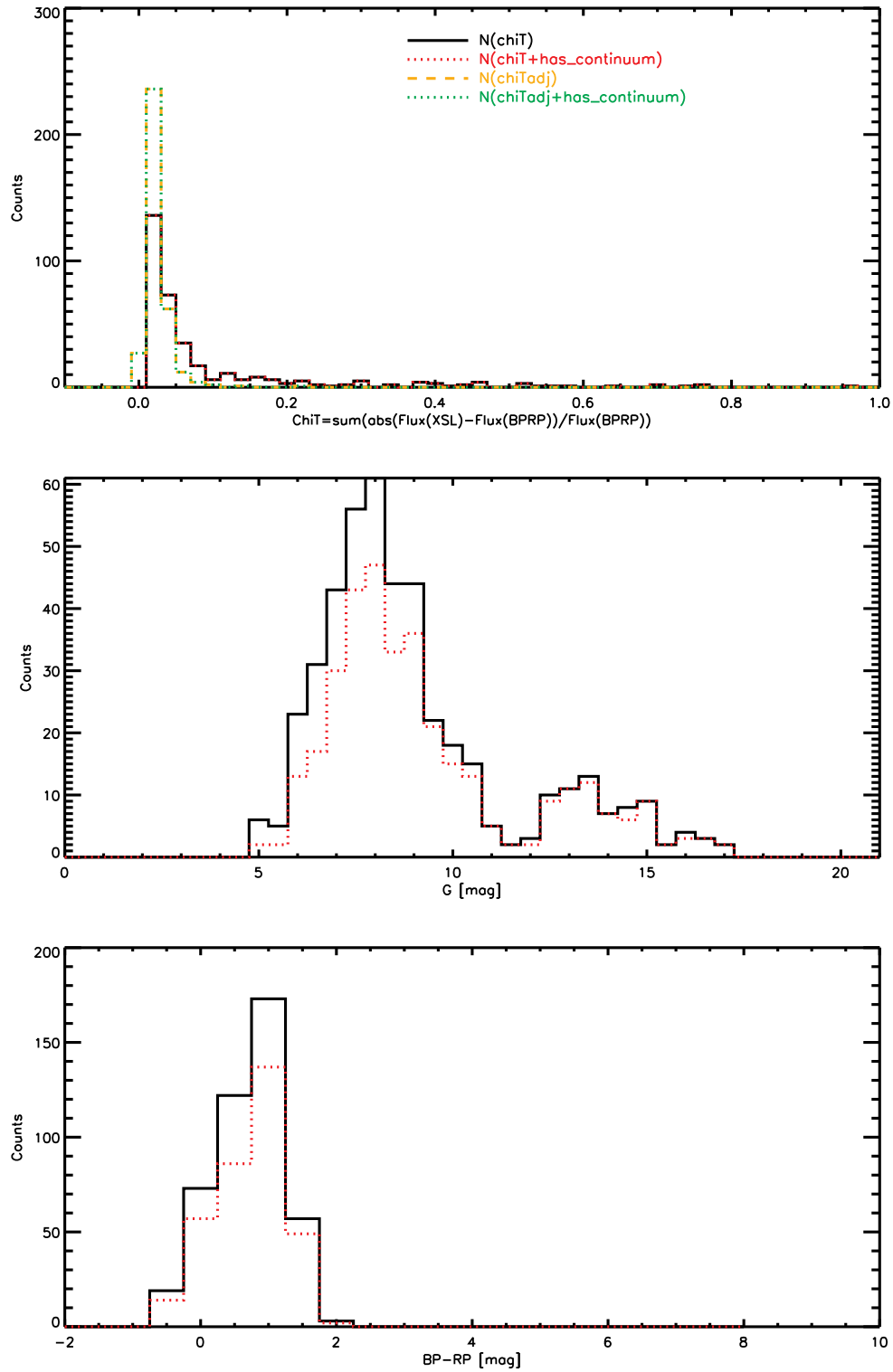


**Fig. 2.** XSL spectra: *Top panel:* Histogram of the  $\chi T$  parameter in black or in red when only considering the data points with `has_xp_continuous='true'`. The histogram of the  $\chi T_{\text{adj}}$  parameter is overplotted in orange or green when only considering the data points with `has_xp_continuous='true'`. *Middle panel:* Histogram of the G magnitudes. In red the histograms of those sources with `has_xp_continuous='true'`. *Lower panel:* Histogram of the BP-RP colors. In red the histograms of those sources with `has_xp_continuous='true'`.

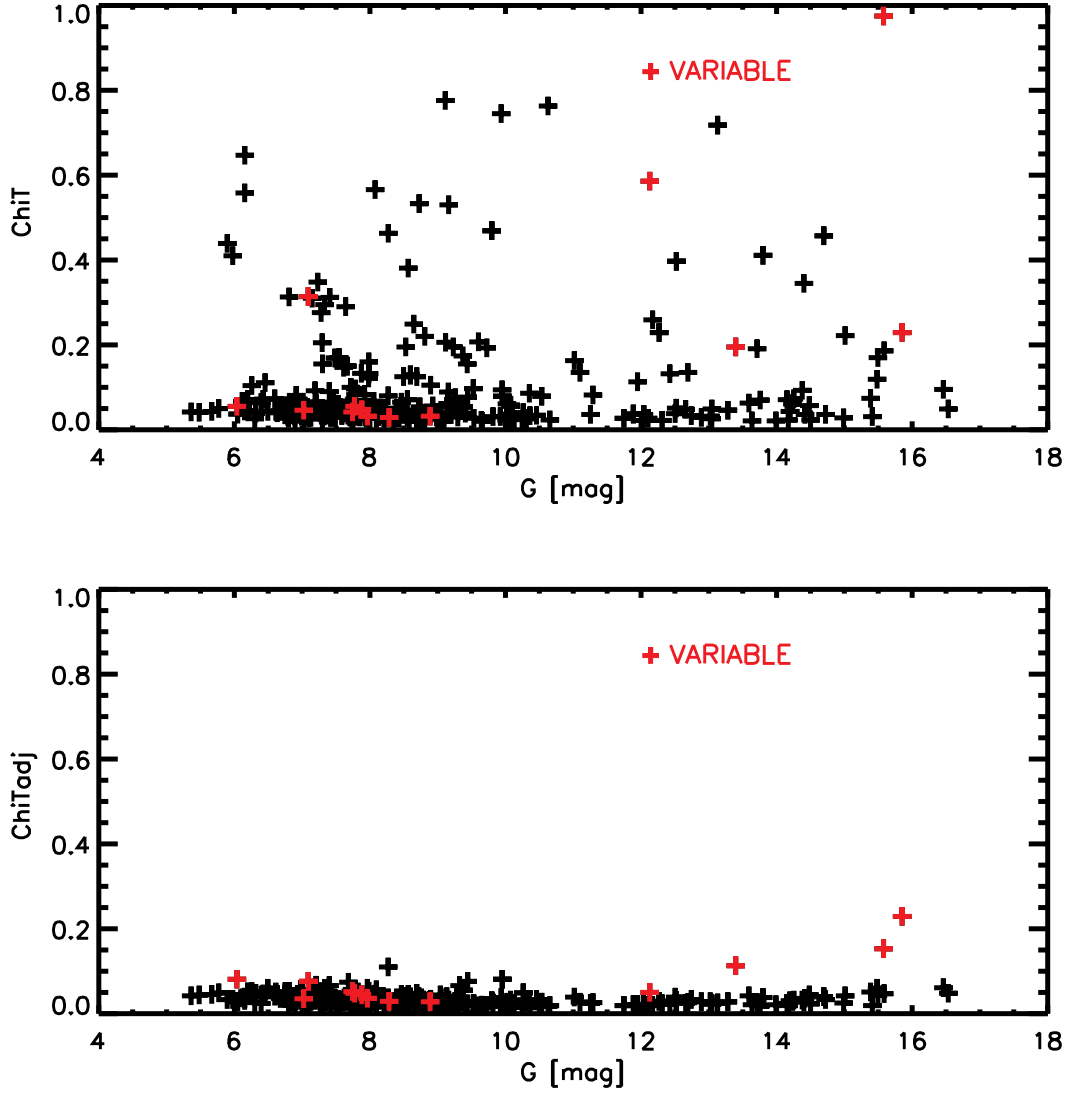


**Fig. 3.** *Upper panel:*  $\chi_i T$  versus  $G$ mag of the XSL stars. *Lower panel:* An adjusted  $\chi_i T$ , i.e. a  $\chi_i T$  run after a small rescaling of the XSL spectrum.

## 2.2 Matching parameters: fact, $\chi_i T$ , and $\chi_i T_{adj}$

The  $\chi_i T$  parameter is defined as:  $\chi_i T = \sum \frac{flux(XSL) - flux(BPRP)}{flux(BPRP)} / N_{bin}$ . and is a measure of the quality of the spectral match. The “fact” (short for factor) parameter is simply the average ratio of the flux(BP/RP) and the flux(XSL) between 650 and 850 nm. It ranges from 0.5 to 4.5. In Fig. 11, the fact values are plotted versus the  $\chi_i T$  values. There is a clear correlation between the fact values and  $\chi_i T$  values. A  $\chi_i T$  value of about 0.5 corresponds to a factor 2, while 0.75 corresponds to a factor 4. The  $\chi_i T$  is a measure of the percentage of deviations between the two flux density vectors. This suggests that the XSL spectra have random (but constant) percentage errors in their flux densities (from a factor 0.5 to a factor 4.5). A  $\chi_i T_{adj}$  is calculated after having

rescaled the flux density vector ( $flux(XSL) \cdot fact$ ); the  $\chi_i T_{adj}$  values have a much narrower range from 0 to 0.1. Possible real bias/trends between residuals and colors/magnitudes/spectral types can be detected only by correlating the  $\chi_i T_{adj}$  values with the stellar parameters (after correcting for the random percentage errors). By being a constant factor, in the plane  $\log(F_\lambda)$  versus  $\lambda$ , the shape of the spectrum is preserved. In Fig. 2, the histogram of the  $\chi_i T_{adj}$  values is seen to peak around 0.025. In Figs. 3 and 4, the  $\chi_i T$  and  $\chi_i T_{adj}$  values are plotted versus the  $G$ -mag and the BP-RP color.

A  $\chi_i 2$  parameter is also calculated,  $\chi_i 2 = 1/(N - 1) \times \sum \frac{(flux(XSL) - flux(BPRP))^2}{Err_{flux(XSL)}^2 + Err_{flux(BPRP)}^2}$ . Analogously to the  $\chi_i T$  and  $\chi_i T_{adj}$  parameters, a  $\chi_i 2$  and a  $\chi_i 2_{adj}$  are calculated (see Figs. 11).

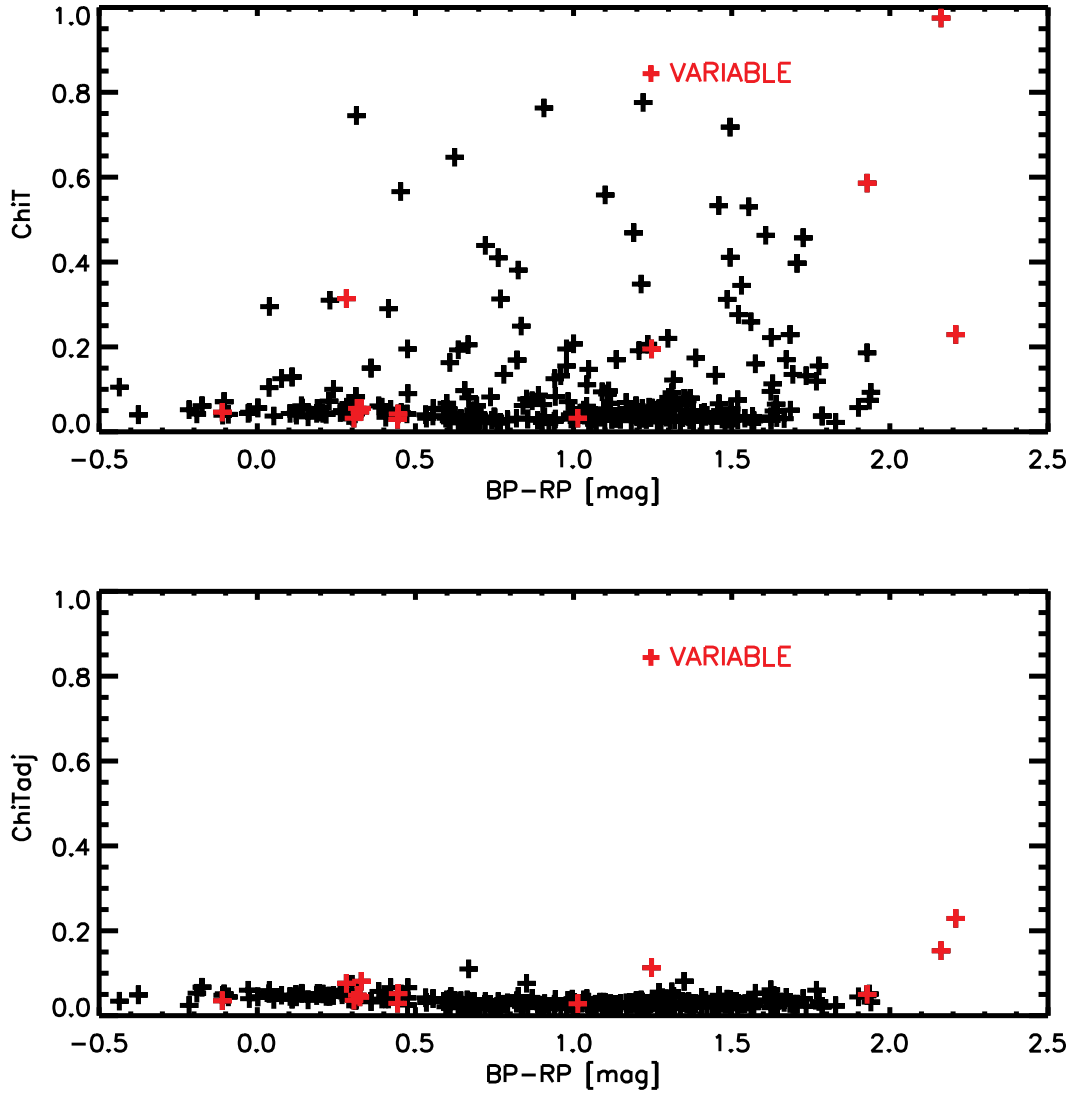


Fig. 4. *Upper panel:*  $\chi_i T$  versus BP-RP mag of the XSL stars. *Lower panel:* An adjusted  $\chi_i T$ , i.e. a  $\chi_i T$  run after a small rescaling of the XSL spectrum.

All sources with a BP/RP spectrum have more than 15 observations in BP and RP bands (Figs. 6 and 7).

By selecting those XSL spectra which have deviations within 1% from the Gaia RP spectra ( $\chi_i T < 0.1$ , and  $0.99 < \text{ratioR} < 1.01$ ) and that are single stars and non variable, a list of optimal 50 XSL stars is obtained.

A search on SIMBAD to exclude variables, binaries, and peculiar emission line stars yields information for 301 stars out of 345 with BP/RP spectra. Eventually, by retaining those spectra with flag OK from SIMBAD and with fitting deviations within 1% from the Gaia DR3 RP spectra 24 spectra are selected, which are listed in Table 2. These 24 XSL spectra may help to assess the quality of the BPRP spectra below 400 nm. Indeed, the residuals of the fit have a much larger scatter when the stars

are redder than BP-RP=1.2 mag and fainter than G=10.5 mag (Figs. 8, 9).

A csv table with the 447 XSL entries, which lists the XSL IDs, Gaia IDs, the flag OK from SIMBAD, and the DR3 quality fit (1 id within 1% of the flux) is located here.

### 3 XSL and SPSS

The 3 matches between the XSL library and the SPSS are listed in Table 1, and the spectra are shown in Fig. 10. As found when comparing BPRP spectra and XSL spectra, the three XSL spectra of Feige 110 differ in their continuum levels. When compared to the SPSS spectrum, the XSL flux zeropoint appears to be up to 50% off.

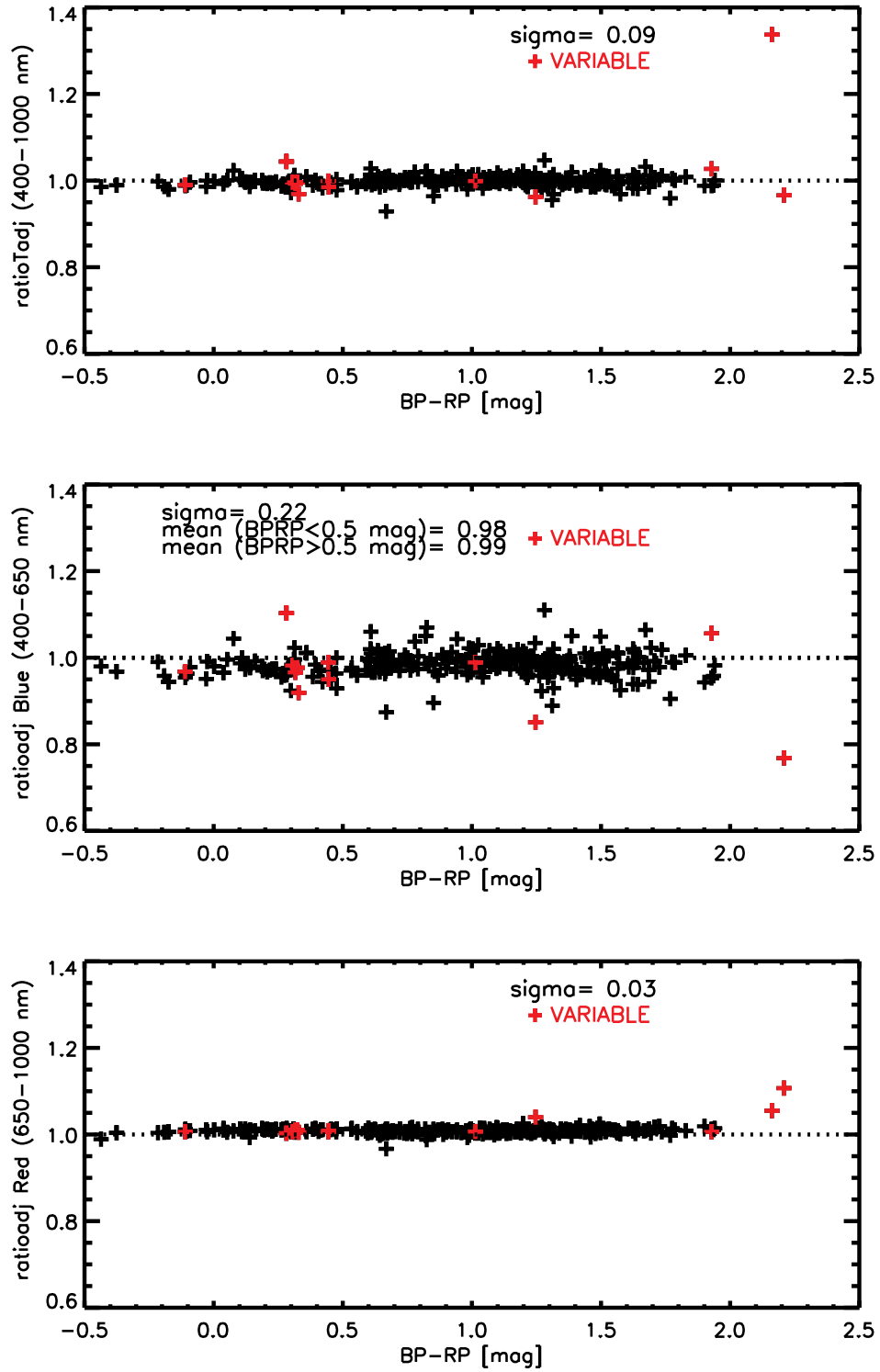


**Fig. 5.** XSL spectra: the residual with the Gaia DR3 BP/RP spectra are smaller in the red part of the spectrum (650-1000 nm), giving a smaller chiadj, than in the blue part (400-650 nm).

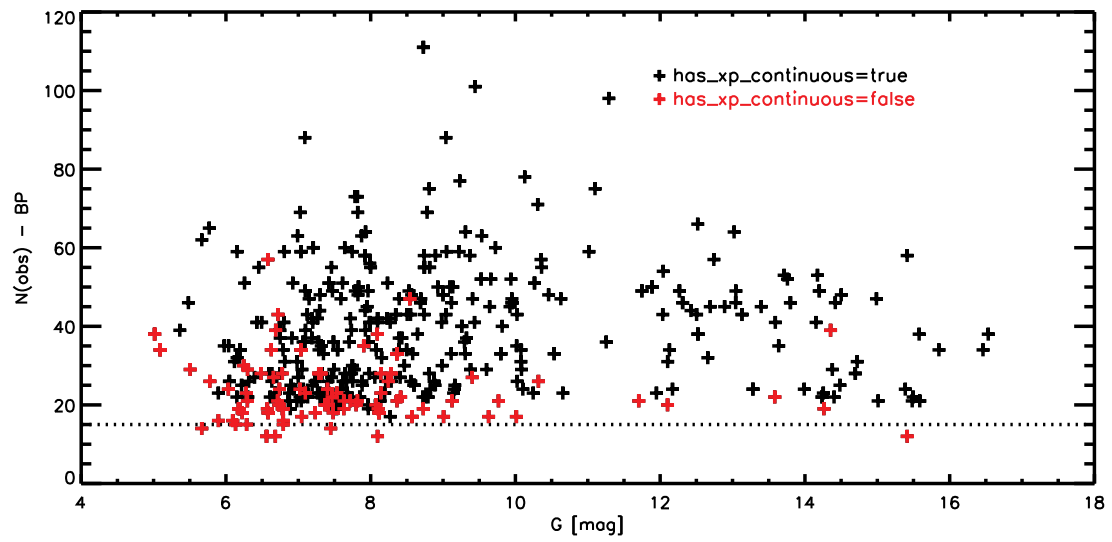


Fig. 6. XSL stars: Number of observation in BP-band versus Gmag.

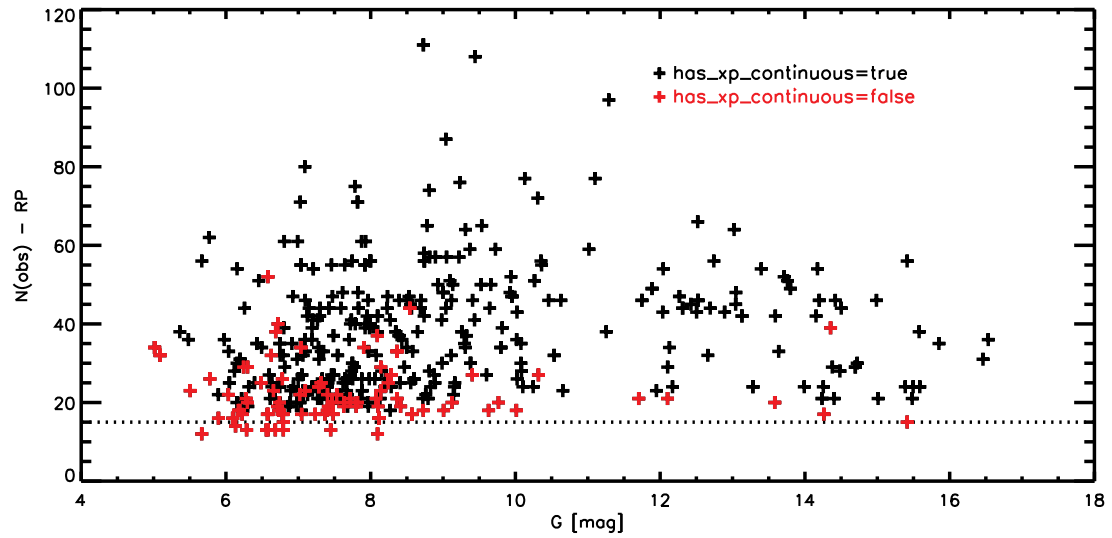
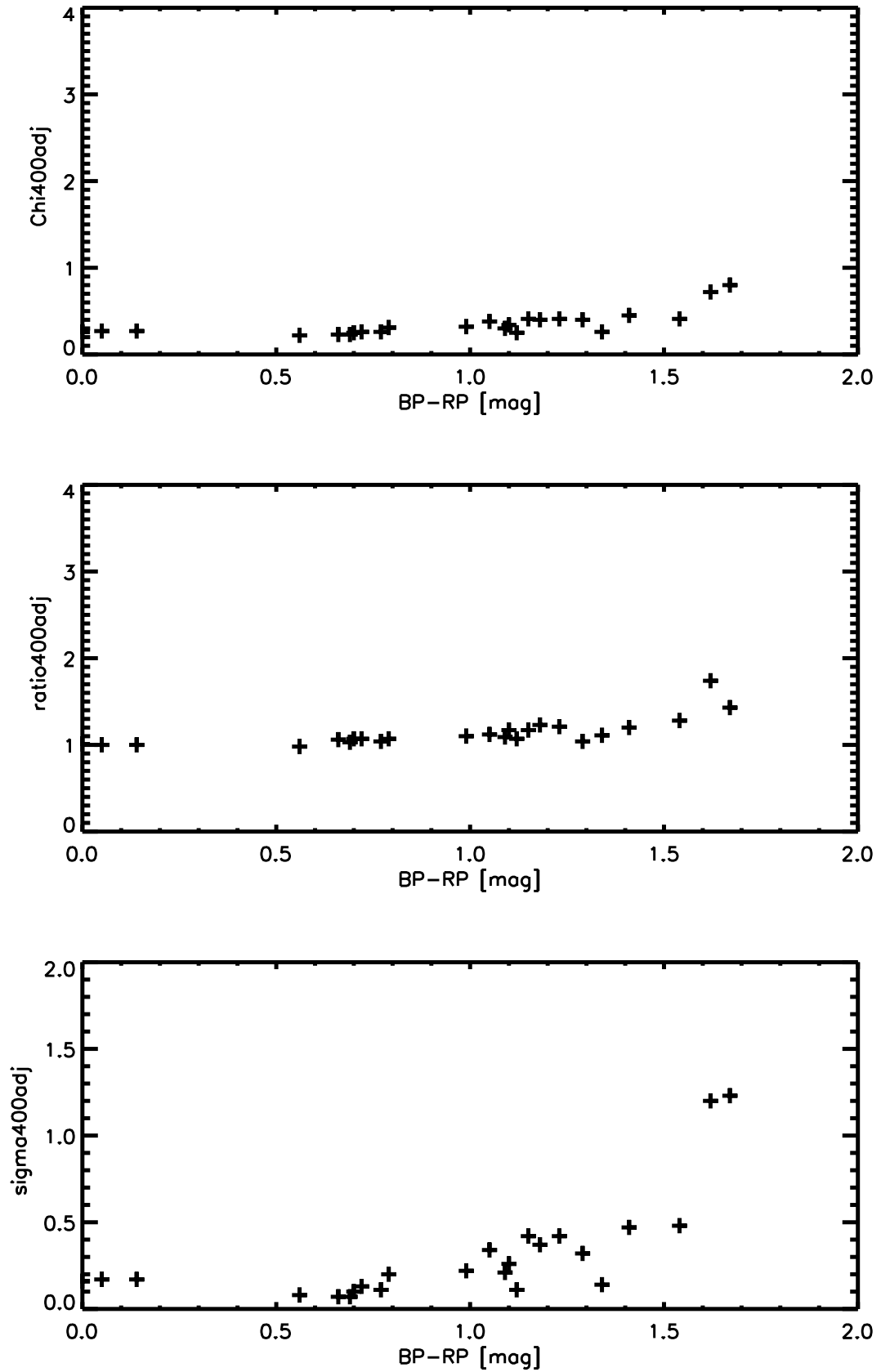


Fig. 7. XSL stars: Number of observation in RP-band versus Gmag.

**Table 1.** Three matches found between the XSL spectra and those from the SPSS library.

Gaia-DR3 ID	XSL	SPSS	SPSS_ID	fact
2633603478379307904	X0758	23	Feige110	0.894
2633603478379307904	X0766	23	Feige110	0.985
2633603478379307904	X0790	23	Feige110	1.976



**Fig. 8.** XSL stars: Using the best sample of 24 XSL spectra (with adjusted slope), the performance of the fit below 400 nm is analyzed. There is clearly a much larger scatter for stars redder than  $BP-RP=1.2$  mag.



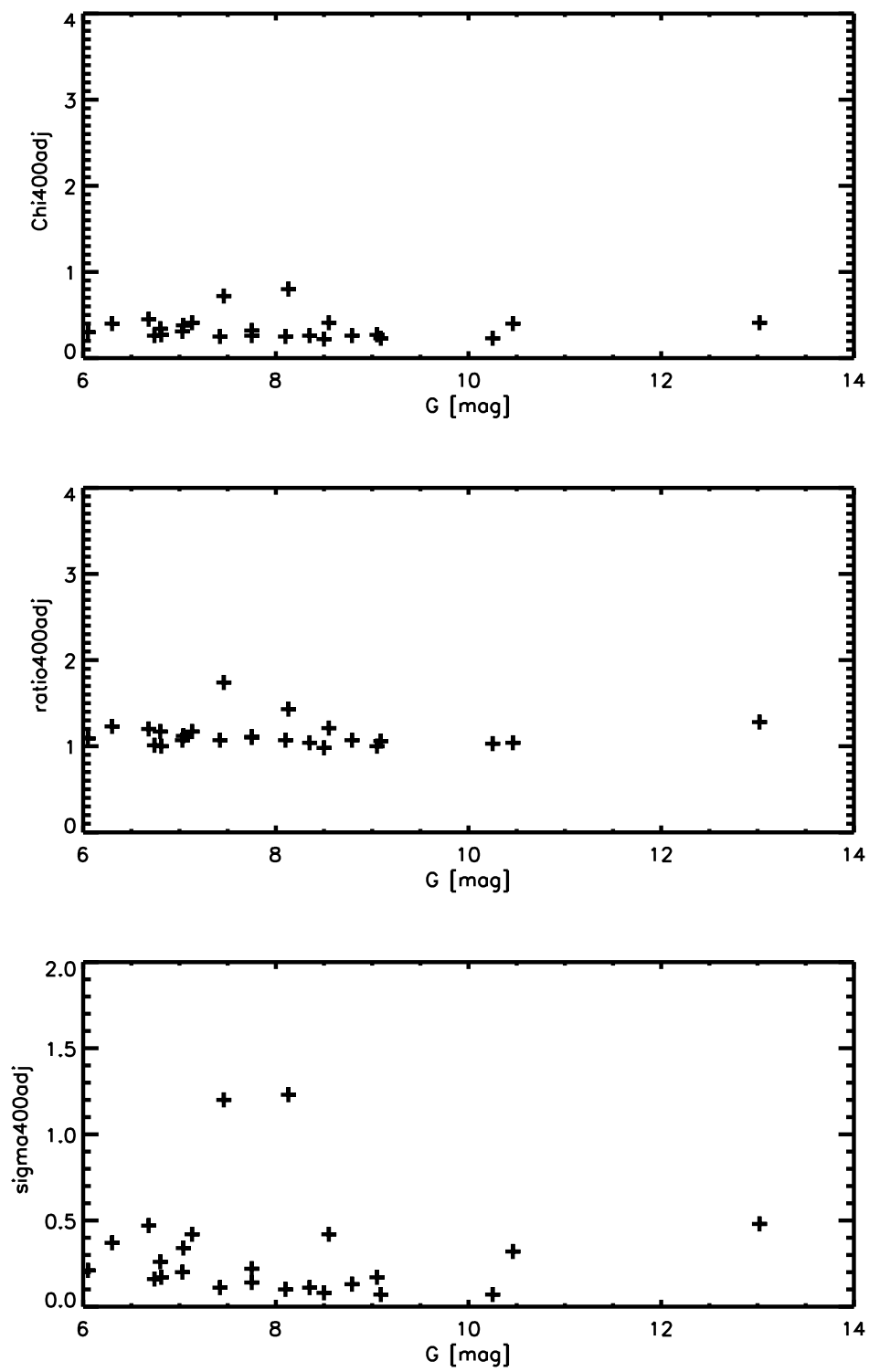


Fig. 9. XSL spectra.

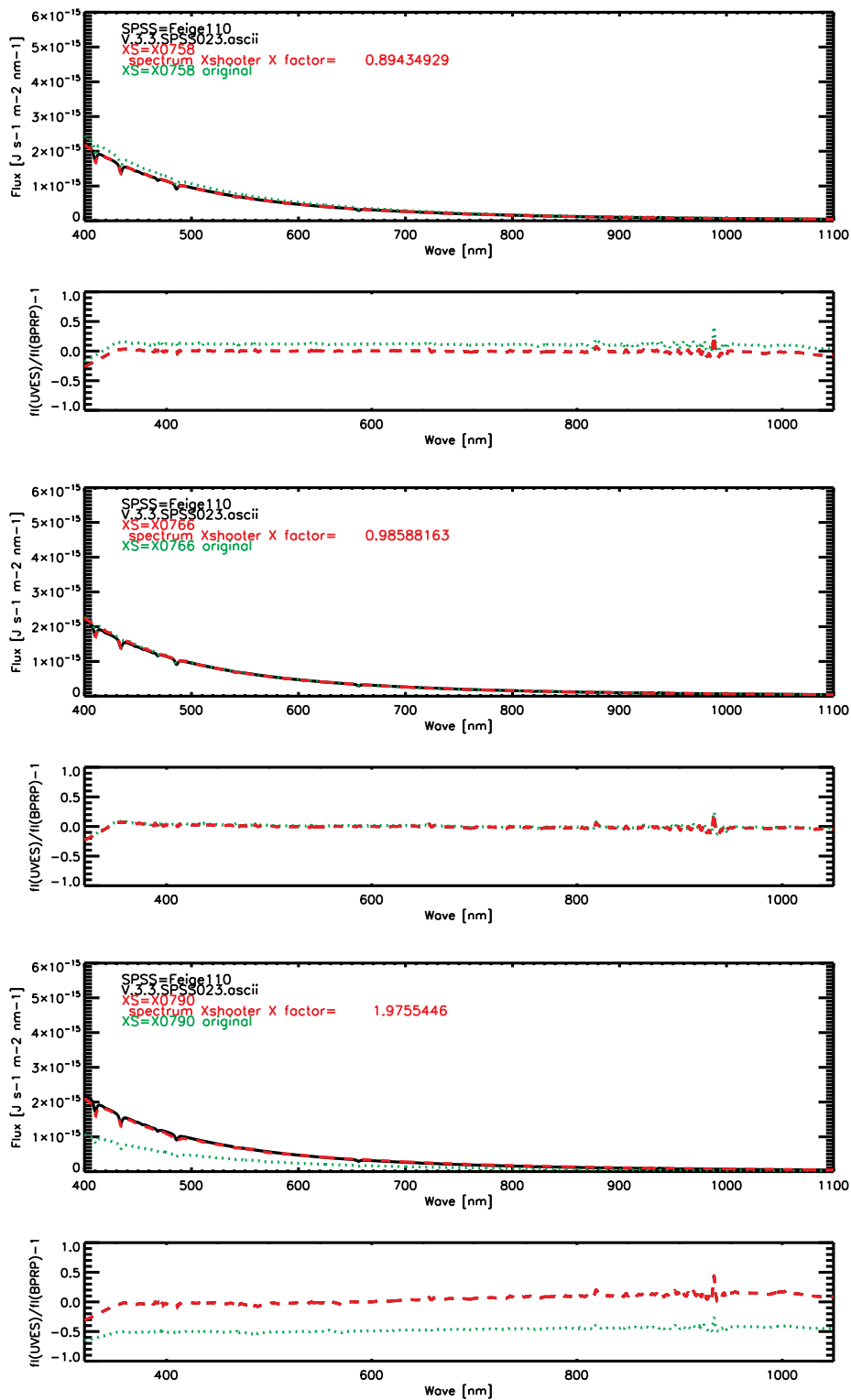


Fig. 10. Overlay of the 3 XSL spectra of Feige110 with its SPSS spectrum.

**Table 2.** Final list of 24 best spectra (out of the 345 matches found between the Best-selected XSL spectra and the Gaia DR3 BP/RP library).

Gaia ID	XSL	G [mag]	BP-RP [mag]	fact	chiadj	chiadjB	chiadjR	ratioB	sigmaB	ratioR	sigmaR
52624073910834176	X0072	9.093	0.657	0.995	0.020	0.025	0.013	1.006	0.040	1.003	0.020
6916198691587462272	X0177	7.747	0.995	0.989	0.028	0.038	0.018	0.986	0.049	1.009	0.026
2699301565882761344	X0179	8.345	0.769	0.996	0.021	0.028	0.013	0.990	0.036	1.002	0.021
6905364821265383424	X0195	6.048	1.095	0.979	0.028	0.039	0.017	0.976	0.048	1.012	0.027
4246840611198113024	X0196	6.743	0.002	0.984	0.044	0.050	0.026	0.980	0.096	1.011	0.063
6858374206854249728	X0200	8.096	0.703	0.991	0.022	0.030	0.012	0.983	0.033	1.007	0.020
4308878561939677824	X0207	6.679	1.414	0.976	0.036	0.058	0.023	0.960	0.069	1.013	0.032
1820374029621976704	X0211	7.422	1.121	0.986	0.025	0.033	0.019	0.991	0.044	1.010	0.030
1833199729671740800	X0212	7.036	1.045	0.980	0.028	0.040	0.016	1.000	0.068	1.011	0.023
3636549599797661824	X0378	10.458	1.294	0.997	0.033	0.057	0.017	0.954	0.065	1.011	0.023
2722849325377392384	X0445	10.245	0.693	0.987	0.017	0.021	0.012	0.992	0.028	1.005	0.018
4158615798208505472	X0449	7.751	1.338	0.989	0.020	0.030	0.013	0.988	0.037	1.003	0.020
4469871906338470528	X0450	6.812	0.142	0.993	0.052	0.063	0.024	0.977	0.110	1.010	0.057
2957939686088825472	X0522	13.022	1.542	0.986	0.028	0.048	0.017	0.956	0.051	1.011	0.024
3122668346360478976	X0578	6.799	1.099	0.997	0.027	0.038	0.017	1.000	0.067	1.003	0.027
3316978400610184832	X0581	6.301	1.182	0.998	0.026	0.039	0.016	1.007	0.076	1.006	0.024
3124790609962295552	X0583	7.129	1.148	1.002	0.029	0.045	0.016	1.002	0.081	1.003	0.023
5617564477239812864	X0585	7.026	0.792	0.999	0.026	0.035	0.016	1.003	0.052	1.006	0.025
3142916535882924416	X0588	7.459	1.624	0.985	0.033	0.055	0.022	1.020	0.134	1.008	0.031
6149244697914619392	X0614	9.048	0.052	1.002	0.038	0.042	0.026	0.996	0.106	1.005	0.065
4426498680874318592	X0636	8.505	0.555	1.005	0.040	0.055	0.017	0.959	0.044	1.004	0.028
3232901636947366656	X0772	8.550	1.230	1.001	0.029	0.043	0.018	0.982	0.066	1.007	0.027
3169175179954291968	X0846	8.792	0.721	1.003	0.024	0.028	0.018	0.994	0.038	1.005	0.024
3890172886119687680	X0880	8.129	1.666	1.001	0.031	0.053	0.020	0.989	0.134	1.008	0.029

fact = average ratio of the flux(BP/RP) and the flux(XSL) between 650 and 850 nm.

chiadj =  $\sum \frac{flux(XSL) \times fact - flux(BPRP)}{flux(BPRP)} / Nbin$  from 400 to 1000 nm.

chiadjB =  $\sum \frac{flux(XSL) \times fact - flux(BPRP)}{flux(BPRP)} / Nbin$  from 400 to 650 nm.

chiadjR =  $\sum \frac{flux(XSL) \times fact - flux(BPRP)}{flux(BPRP)} / Nbin$  from 650 to 1000 nm.

ratioBadj = average ratio of the  $flux(BPRP)$  and the  $flux(XSL) \times fact$  between 400 and 650 nm.

sigmaBadj = sigma of the ratios between 400 and 650 nm.

ratioRadj = average ratio of the  $flux(BPRP)$  and the  $flux(XSL) \times fact$  between 650 and 1000 nm.

sigmaRadj = sigma of the ratios between 650 and 1000 nm.

## 4 UVES\_POP

For the UVES\_POP spectra, Names, coordinates, and Gaia IDs were read from the fits header. The reported Gaia IDs were a mix of Gaia DR2 IDs and Gaia DR3 IDs. The annotated target coordinates were up to 2'' off. By using the Names (mostly HD-names) coordinates were retrieved from Simbad. By cross-correlations, 2MASS-IDs, Gaia DR3 IDs, and Gaia DR2 IDs were re-retrieved. A few new matches were located, as listed in Table 3. The other matches were all fine (besides the DR2 and DR3 ambiguity).

### 4.1 UVES\_POP Gaia BP/RP

There are 406 fits available in the UVES\_POP library (Borisov et al. 2022). 376 of them have a Gaia DR3 match. In the table gaiadr3.astrophysical\_parameters, 302 Gaia DR3 matches are found to have has\_xp\_continuous=true. 302 BP/RP mean spectra in the continuous representation could be retrieved and resampled. The UVES\_POP spectra are distributed with a constant bin in wavelength.

UVES\_POP spectra are resampled to the Gaia BP/RP resolution, and compared with the Gaia BP/RP spectra. A  $\chi T$  parameter is calculated as the  $\sum \frac{\text{flux}(\text{UVES\_POP}) - \text{flux}(\text{BPRP})}{\text{flux}(\text{BPRP})}$ . The histogram of the obtained  $\chi T$  is shown in Fig. 12. The Table 4 lists a “factor” which is simply the ratio of the average flux(BP/RP) and average Flux(UVES\_POP) between 650 and 850 nm.

In Figs. 13 and 14, the  $\chi T$  and  $\chi T_{\text{adj}}$  values are plotted versus the G-mag and the BP-RP color. The variables are shown in red, they have a similar distribution as the non-variable stars. The sample comprises a large number of stars brighter than G=4.5 mag, which is the saturation limit for the short-wavelength side of the BP spectrum.

All sources with a BP/RP spectrum have more than 15 observations in BP and RP bands (Figs. 15 and 16). The sources were inspected on SIMBAD and a flag 'OK' was given to stars not variable, not binary.

Stars with the BP/RP flux density vectors within 1% between 650 and 850 nm, ( $\chi T < 0.1$ , and  $0.99 < \text{ratioR} < 1.01$ ), single stars, non-variable, with G> 4. mag, and with the SIMBAD flag='OK' are selected. The list contains 24 spectra (Table 4).

With the best sample, the fit below 400 nm are analyzed and the same trends seen with the XSL library are identified. The residuals of the fit have a much larger scatter when the stars are redder than BP-RP=1.0 mag (Figs. 17 and 18).

A csv table with the 406 UVES entries, which lists the UVES IDs, Gaia IDs, the flag OK from SIMBAD, and the DR3 quality fit (1 is set if the flux is within 1%) is located [A here](#).

## 5 UVES\_POP and SPSS

No matches with the SPSS library were found.

**Table 3.** UVES\_POP library. New identified Gaia-DR3 matches.

Name	Gaia-ID paper	Gaia DR3 ID re-retrieved	2MASS-ID
Castor	none	892348694913501952	07343598+3153184
HD020010	none	5059348952161258624	03120443-2859156
HD036646	none	3217181124645104384	none
HD066811	none	5534788672055388032	08033506-4000112
HD080404	none	5300300156538723328	09170540-5916308
HD083368	none	5410092611674819840	09362541-4845042
HD105113	none	3466217935643483392	12060519-3257402
HD120709	none	6170485544575679104	13514960-3259387
HD145792	none	6049891517263095168	16134549-2425196
HD154873	none	5950941488064653056	17102084-4644182
HD162306	none	4040709497081178496	17515522-3504577
HD162587	none	4040799485267855232	17532345-3453424
IC2391_47	none	5318309534208474112	08461506-5307444

**Table 4.** Final list of 24 best spectra (out of the 302 matches found between the UVES\_POP spectra and the BR/RP spectra).

Gaia ID	XSL	G [mag]	BP-RP [mag]	fact	chiadj	chiadjB	chiadjR	ratioB	sigmaB	ratioR	sigmaR
5065109121778224768	HD018466	6.153	0.704	0.989	0.036	0.051	0.015	1.033	0.081	1.011	0.025
4766376347995853056	HD037227	6.670	0.501	0.997	0.031	0.037	0.020	1.023	0.063	1.010	0.035
5605851482951097600	HD058377	6.754	-0.200	0.987	0.038	0.043	0.021	1.024	0.061	1.013	0.044
5493588665684618752	HD059468	6.548	0.866	0.990	0.032	0.047	0.014	1.044	0.073	1.004	0.022
5586381090520538880	HD059967	6.503	0.807	0.997	0.030	0.043	0.014	1.040	0.062	0.998	0.019
5714859436545926016	HD065810	4.592	0.153	1.024	0.039	0.039	0.038	1.009	0.104	0.983	0.063
5398114596413589120	HD099322	4.969	1.142	0.983	0.033	0.047	0.021	1.052	0.075	1.013	0.026
3516934936698212352	HD109931	5.927	0.430	0.997	0.029	0.032	0.021	1.015	0.066	0.997	0.038
3511640513332581504	HD114642	4.896	0.649	0.999	0.033	0.043	0.017	1.034	0.056	0.998	0.025
6062166950467100032	HD114837	4.788	0.654	0.969	0.044	0.058	0.023	1.031	0.077	1.024	0.036
6092862428844018176	HD125809	6.040	1.377	0.983	0.039	0.054	0.028	1.070	0.088	1.014	0.035
5902781985395901056	HD136351	4.857	0.668	0.992	0.034	0.042	0.021	1.018	0.062	1.018	0.032
5821125860988362752	HD145689	5.933	0.186	0.991	0.042	0.048	0.026	1.020	0.116	1.002	0.057
6777965134807570560	HD198357	5.056	1.541	0.980	0.036	0.059	0.023	1.071	0.121	1.015	0.038
6611824083124944384	HD210111	6.326	0.324	1.006	0.033	0.040	0.018	1.018	0.088	1.004	0.039
6625981669722090112	HD210848	5.458	0.670	1.006	0.028	0.032	0.022	1.022	0.049	1.000	0.032
5318169866178702976	IC2391_8	6.432	-0.113	1.006	0.037	0.041	0.025	1.010	0.093	1.000	0.053
5318083382715884928	IC2391_19	7.292	0.368	1.000	0.033	0.038	0.025	1.023	0.074	0.991	0.042
5318554111133634432	IC2391_23	7.267	-0.008	1.003	0.042	0.046	0.030	1.011	0.122	1.001	0.062
5318499822745556992	IC2391_29	7.370	0.006	1.004	0.044	0.049	0.029	1.009	0.128	0.994	0.062
5318318918726520576	IC2391_41	7.534	0.116	1.003	0.040	0.046	0.026	1.020	0.121	0.996	0.056
5318630973868090496	IC2391_44	9.199	0.529	0.981	0.033	0.042	0.018	1.038	0.060	1.012	0.037
5318327165064125696	IC2391_45	9.371	0.055	1.000	0.035	0.040	0.023	1.013	0.082	0.996	0.050
5318323935248518144	IC2391_46	7.619	-0.085	1.001	0.039	0.042	0.027	1.019	0.076	0.989	0.048

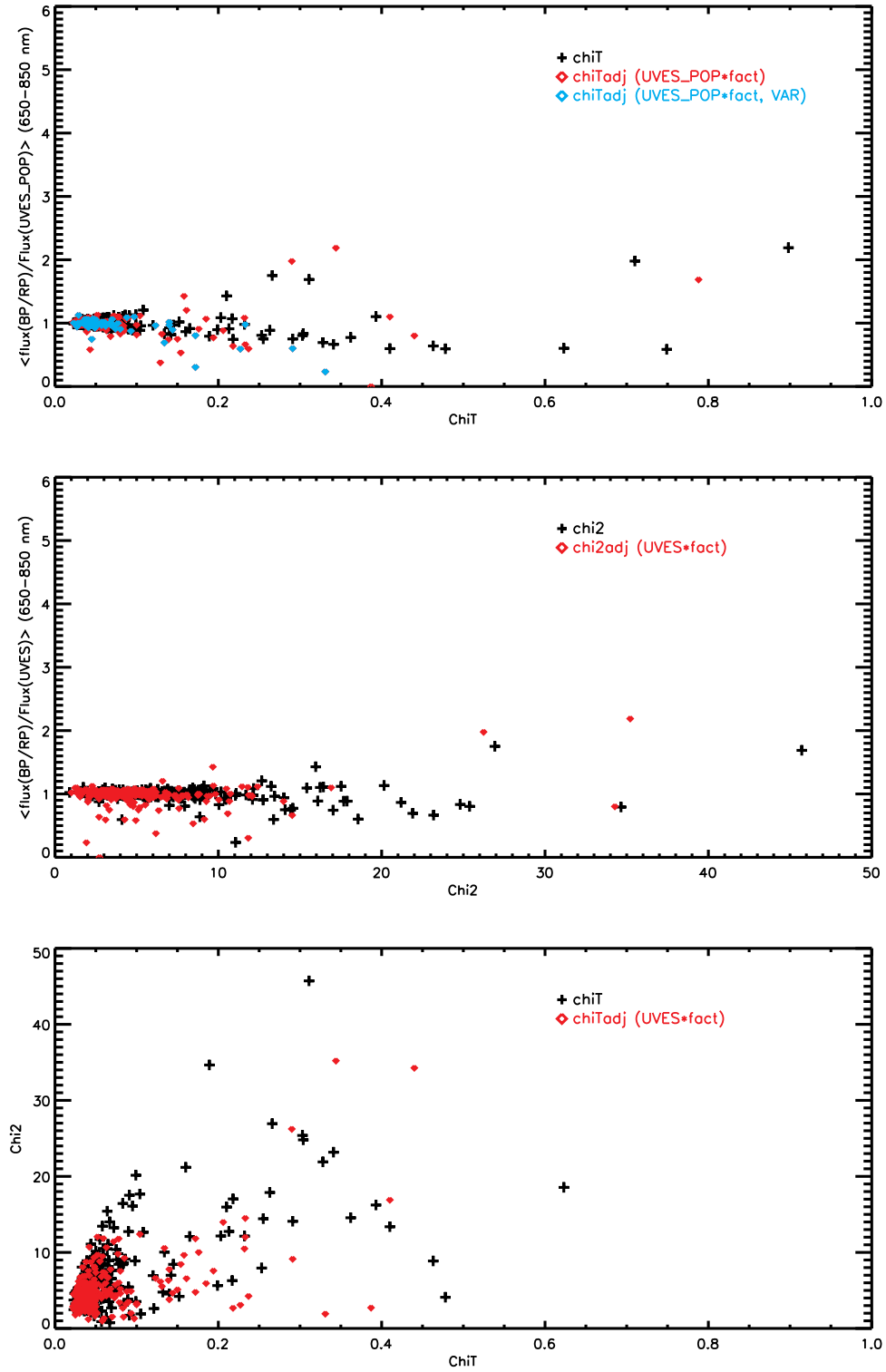


**Fig. 11.** *Upper panel:* UVES: the fact value, i.e., the average flux ratio between 700 and 750 nm (BP/RP) versus the  $\chi^2_{\text{T}}$  values (black plus signs). A  $\chi^2_{\text{Tadj}}$  value is the  $\chi^2_{\text{T}}$  of the modified spectrum  $\text{UVES} \times \text{fact}$ . The  $\chi^2_{\text{Tadj}}$  values are much smaller than the  $\chi^2_{\text{T}}$  values. *Middle panel:* UVES: the fact value, i.e., the average flux ratio between 700 and 750 nm (BP/RP-XSL) versus the  $\chi^2$  values (black plus signs). A  $\chi^2_{\text{adj}}$  value is the  $\chi^2$  of the modified spectrum  $\text{XSL} \times \text{fact}$ . *Lower panel:* UVES: the  $\chi^2_{\text{T}}$  versus the  $\chi^2$  values (black plus signs).

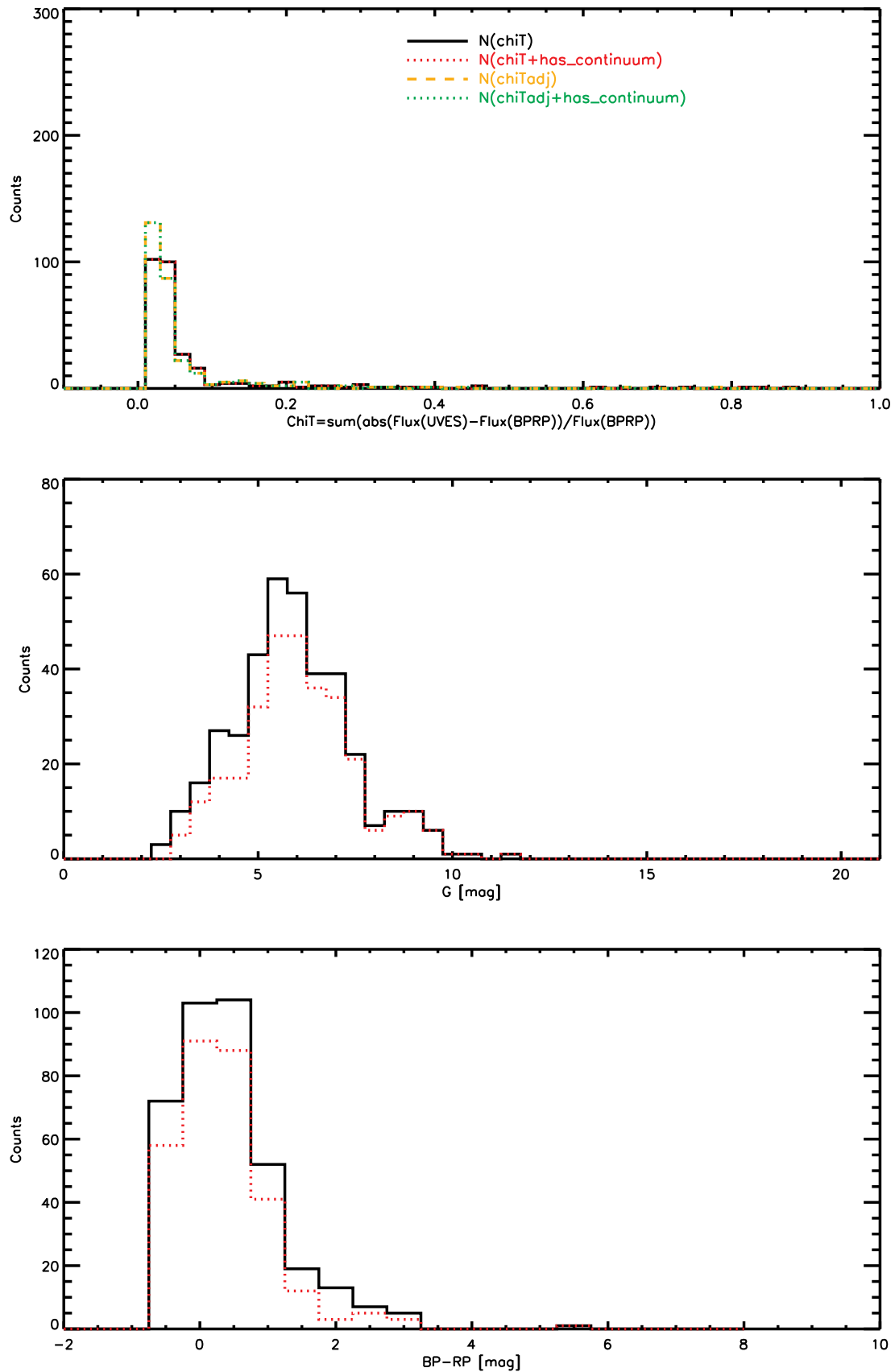


**Fig. 12.** UVES\_POP spectra: *Top panel:* Histogram of the  $\chi T$  parameter. *Middle panel:* Histogram of the G magnitudes. *Lower panel:* Histogram of the BP-RP colors. In red the histograms of those sources with `has_xp_continuous='true'`.

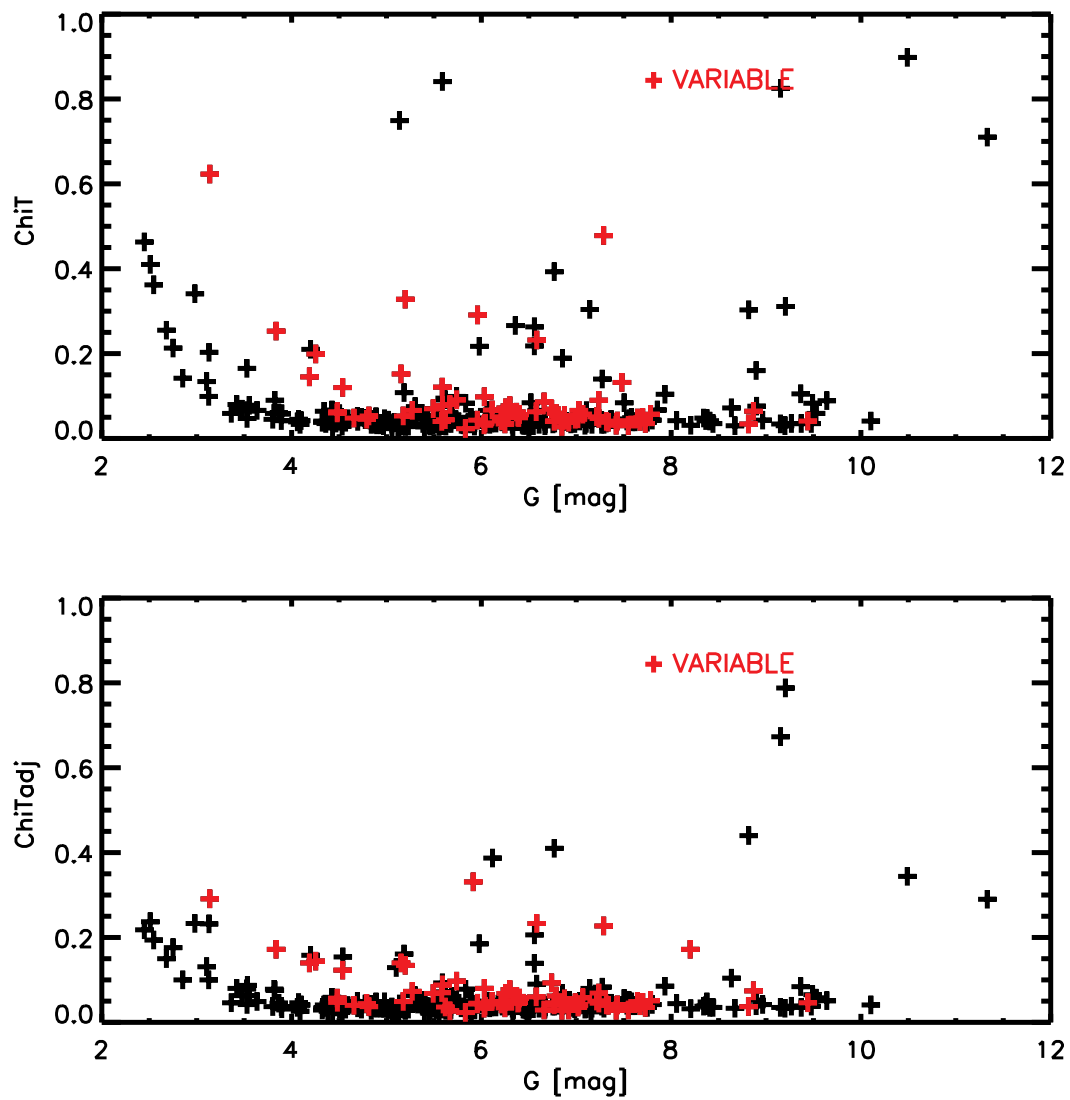


**Fig. 13.** UVES\_POP spectra: *Upper panel:*  $\text{chiT}$  versus  $G$ mag of the UVES\_POP stars. *Lower panel:* An adjusted  $\text{chiT}$ , i.e. a  $\text{chiT}$  run after a small rescaling of the UVES\_POP spectrum.



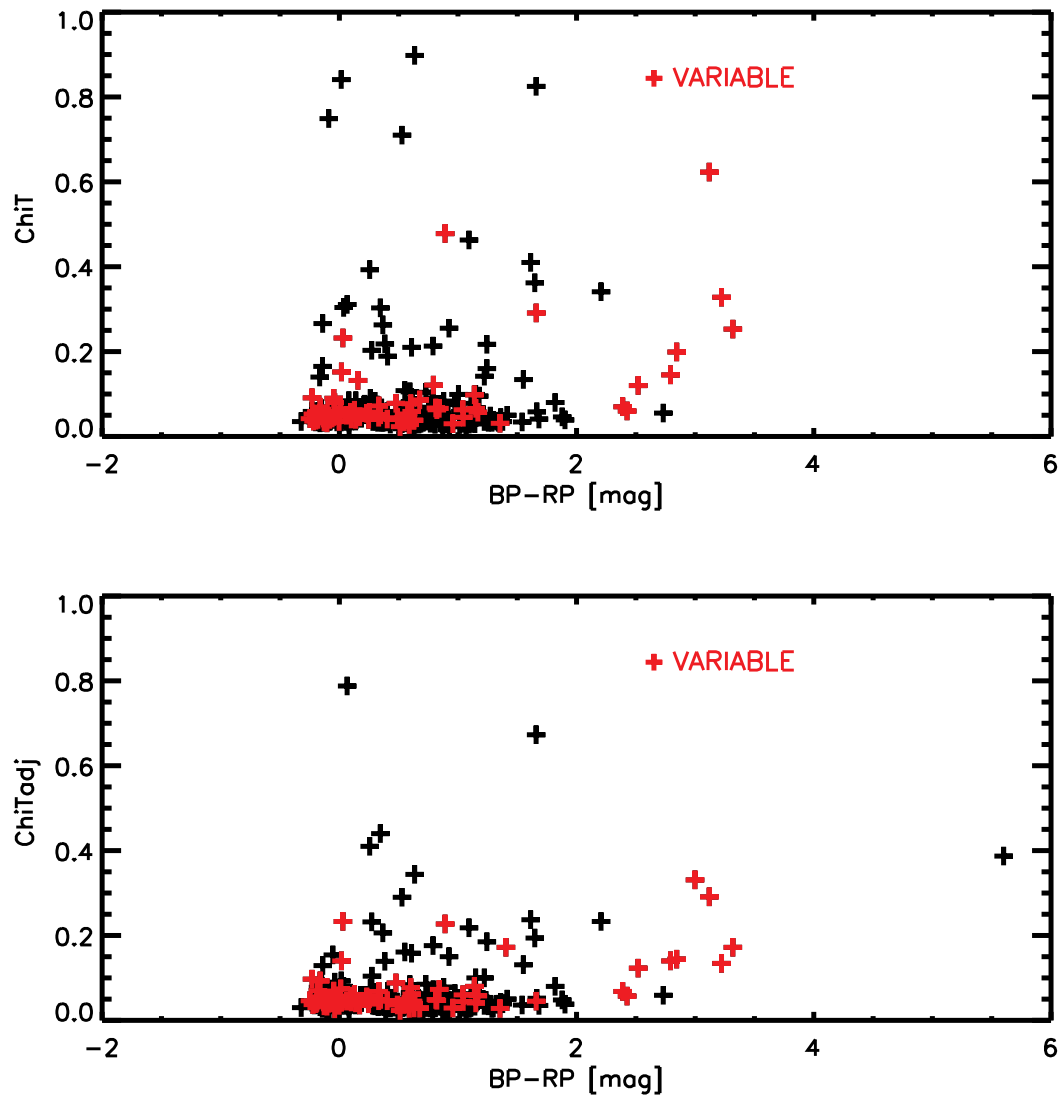


**Fig. 14.** UVES\_POP spectra: *Upper panel:*  $\chi_i T$  versus BP-RP mag of the UVES\_POP stars. *Lower panel:* An adjusted  $\chi_i T$ , i.e. a  $\chi_i T$  run after a small rescaling of the UVES\_POP spectrum.

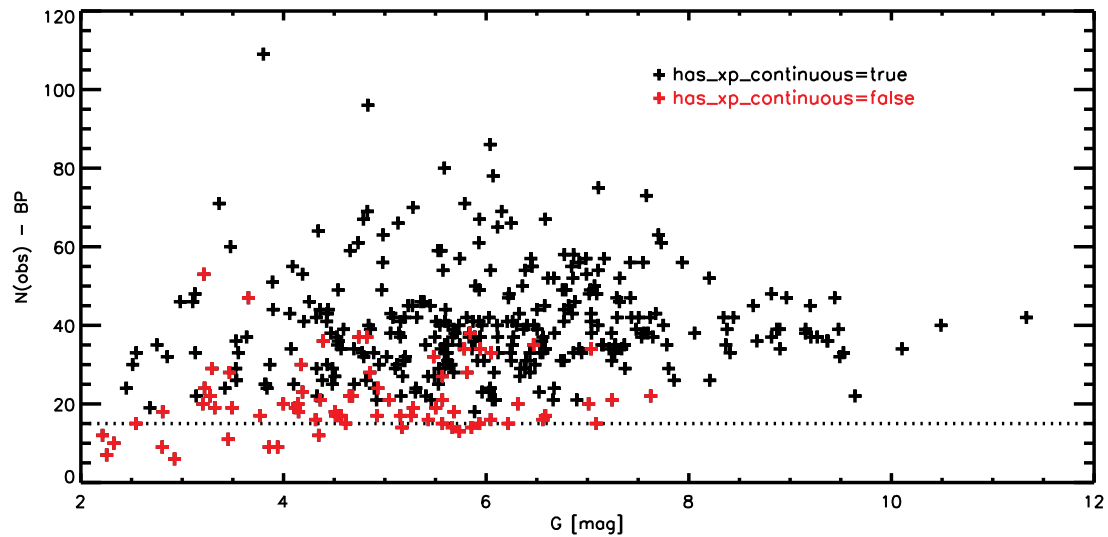


Fig. 15. UVES\_POP spectra: Number of observation in BP-band versus Gmag.

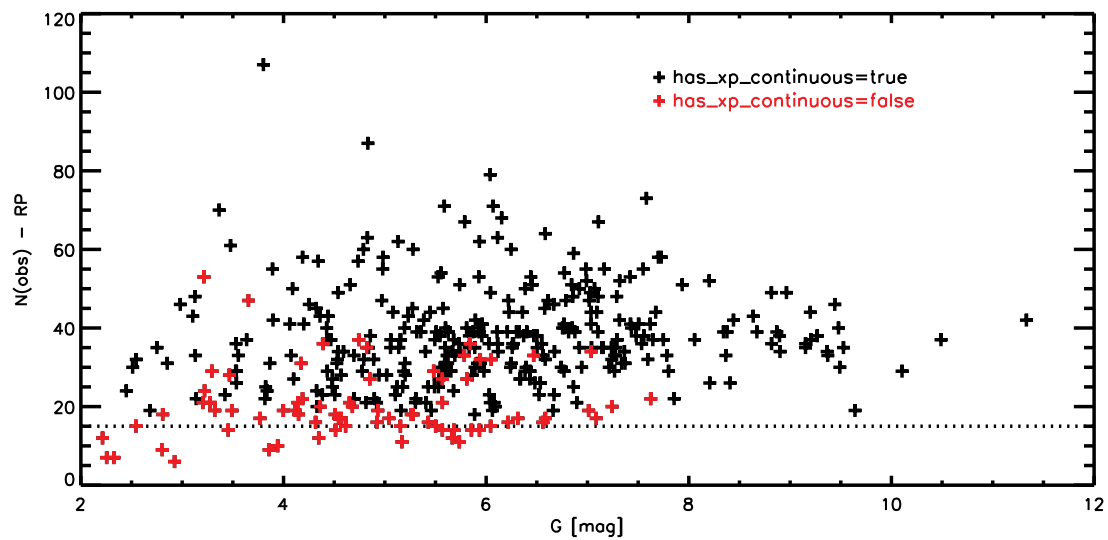
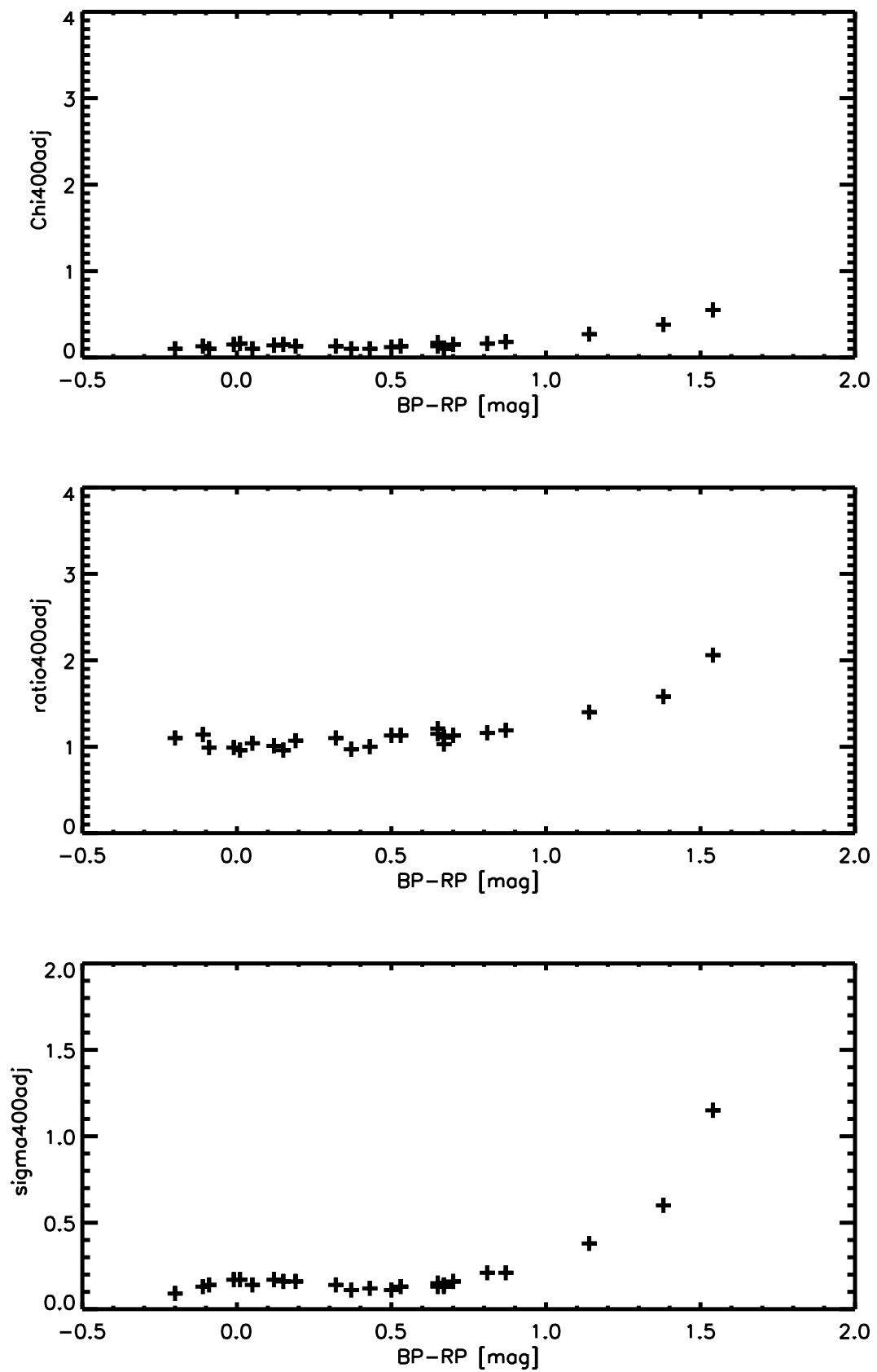
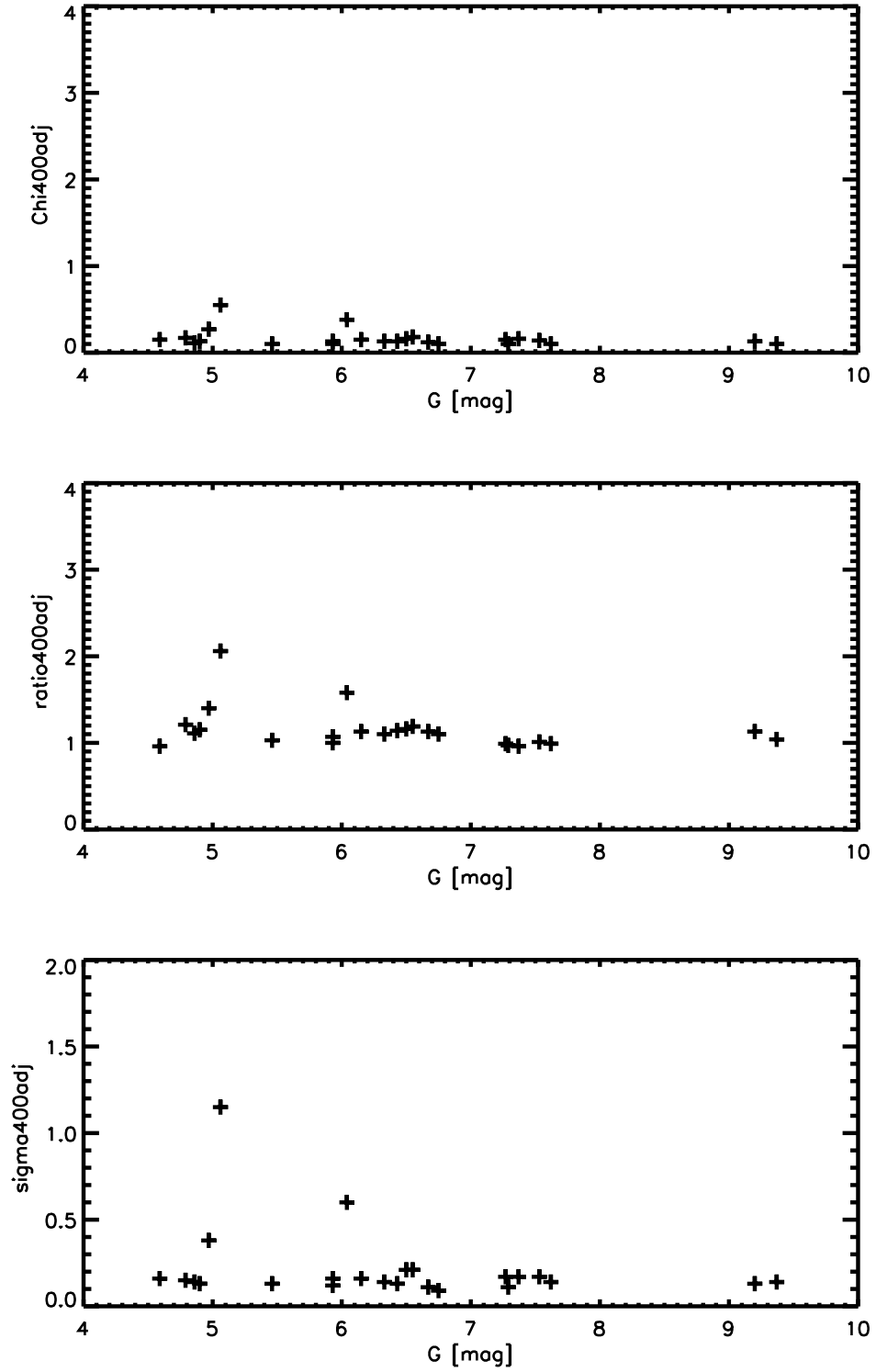


Fig. 16. UVES\_POP spectra: Number of observation in RP-band versus Gmag.



**Fig. 17.** UVES\_POP spectra: Using the best sample of UVES\_POP spectra (with adjusted slope), the performance of the fit below 400 nm is analyzed. There is clearly a much larger scatter for stars redder than  $BP-RP=1.0$  mag.



**Fig. 18.** UVES\_POP spectra: There is no clear trend with the magnitude. The UVES magnitudes are brighter than those of the XSL library.

## 6 NGSL

The Next Generation Spectral Library (NGSL) comprises 513 spectra taken with STIS covering from 0.2  $\mu\text{m}$  to 1.0  $\mu\text{m}$  at a resolving power,  $R=1000$  (Pal et al. 2023). The paper abstract reports 514 stars, and the distributed file, `rmeta_out.csv`, has 514 lines, however, the first line is a header.

Stellar identification names and coordinates were taken from the fits header. A few typos in the names were found by checking by coordinates the entries on SIMBAD. It is assumed that the coordinates are correct and that the names need to be fixed. The name GL109 should be GJ109.

The name GL15A should be GJ15A.

The name HD099481 should be HD99491.

The name HD099492B should be HD099492.

By using the coordinates, automatically 503 2MASS matches within 2.5 were found, and 9 other matches were found on SIMBAD. Only one star does not have a 2MASS entry.

Gaia DR3 matches were found in three steps.

Gaia data points within 1.5 from the 2MASS coordinates were retained as matches (50 matches missing). For the 50 missing matches, Gaia data points associated with the given 2MASS data points were retained.

The remaining 19 missing Gaia matches were examined on SIMBAD and found to be high-velocity stars and binary systems. Seven other GAIA matches were added using the SIMBAD database.

The obtained list of counterparts was verified with SIMBAD and Vizier. There are numerous binary systems, and the automatic Gaia and 2MASS positional matches must be checked. For 3 wide systems, the NGSL spectrum refers to the main component, and the names can be corrected from HD023439, HD015089, HD048279 to HD023439A, HD015089A, HD048279A, which have both 2MASS and Gaia counterparts.

The NGSL spectra of HD025893, HD195434, HD069083, and HD197964, which have nearby companions within 1-3'', refer to the main components HD025893A/Gaia DR3 225709641034907264, HD195434A/Gaia DR3 4245659976227848704, HD069083A/Gaia DR3 5541217413464157696, and gam02 Del/Gaia DR3 1763000413344449792, and have unresolved 2MASS counterparts.

In conclusion, 501 stars out of 513 do have a Gaia DR3 counterpart.

### 6.1 Comparison and residuals plots

For the NGSL library, 381 BP/RP spectra were retrieved. shown in this html page.

The NGSL spectra have a wavelength bin varying from 0.0103 to 0.4884 nm. The spectra were rebinned to the Gaia resolution and compared with it in the plane  $F_\lambda$  versus wavelengths. For the bulk of stars, an excellent agreement is found between the NGSL spectra and the BP/RP spectra. Small constant shifts applied to the  $F_\lambda$  vectors improve the quality of the fit. In general, the BP/RP spectra are brighter than the NGSL spectra, which could be due to an imperfect correction for slit loss, as suggested by Elena Pancino and discussed in Sect. 4.2 of Pal et al. (2023).

255 stars are commented with an "OK" because those are not listed in SIMBAD as a particular type of stars (VAR, emission..) or binary systems, and are not saturated. When also selecting those with best matches with the BP/RP spectra of DR3 (flux deviations within 1%), then this number decreases to 16 The best 16 are displayed on a separate html page and are listed in Table 5.

## 7 NGSL and SPSS

There are no matches with the SPSS library.

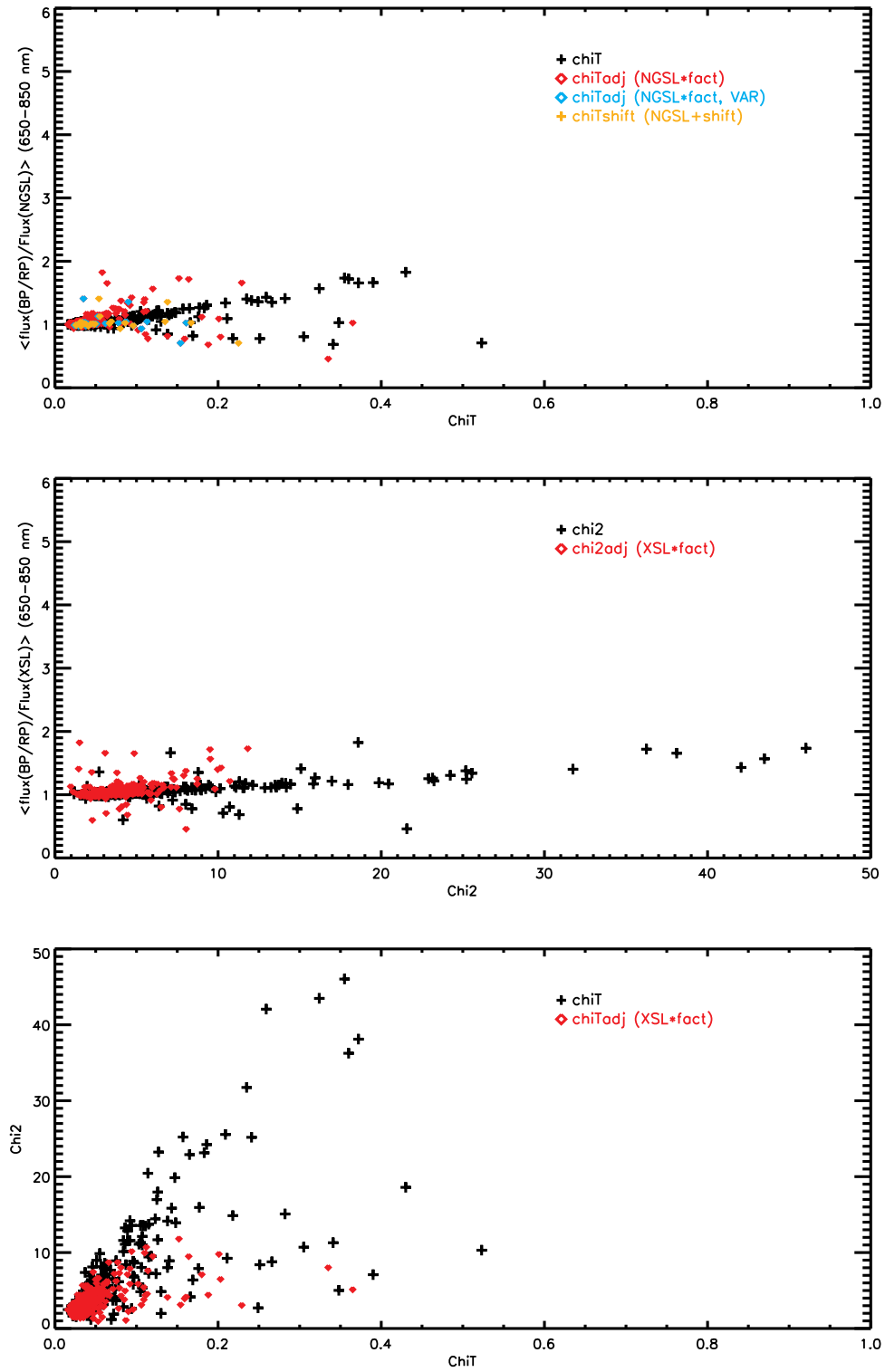


**Fig. 19.** NGSL: the fact value, i.e., the average flux ratio between 650 and 850 nm (BP/RP-NGSL) versus the  $\text{ChiT}$  values (black plus signs). A  $\text{ChiTadj}$  value is the  $\text{ChiT}$  of the modified spectrum  $\text{NGSL} \times \text{fact}$ . A  $\text{ChiTshift}$  value is the  $\text{ChiT}$  of the modified spectrum  $\text{NGSL} + \text{fact}$ . *Middle panel:* NGSL: the fact value, i.e., the average flux ratio between 700 and 750 nm (BP/RP) versus the  $\text{Chi2}$  values (black plus signs). A  $\text{Chi2adj}$  value is the  $\text{Chi2}$  of the modified spectrum  $\text{NGSL} \times \text{fact}$ . *Lower panel:* NGSL: the  $\text{ChiT}$  versus the  $\text{Chi2}$  values (black plus signs).

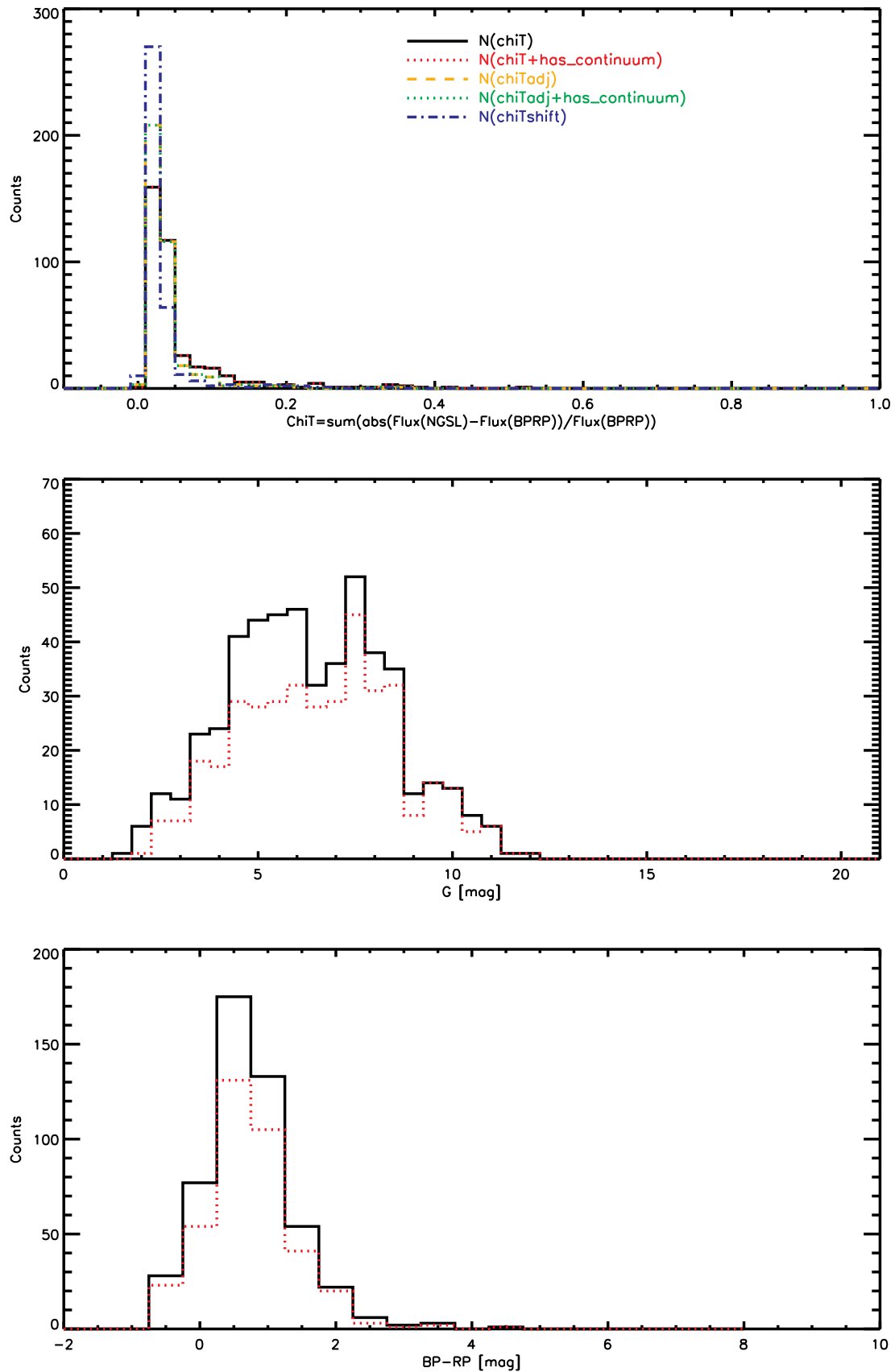


**Fig. 20.** NGSL spectra: *Top panel:* Histogram of the  $\text{chiT}$  parameter. *Middle panel:* Histogram of the G magnitudes. *Lower panel:* Histogram of the BP-RP colors. In red the histograms of those sources with `has_xp_continuum='true'`.

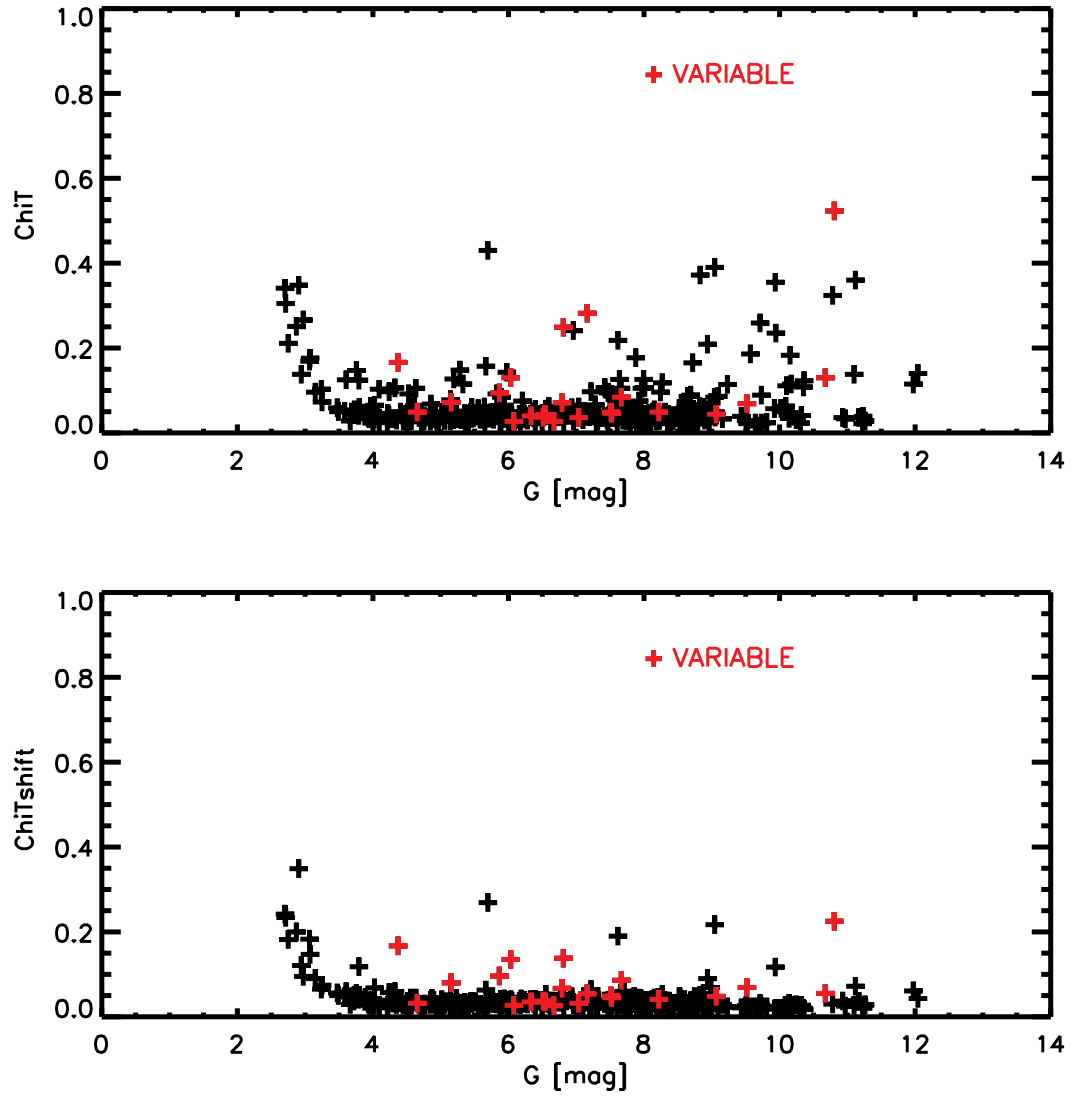


**Fig. 21.** NGSL spectra: *Upper panel:*  $\chi_i T$  versus  $G_{\text{mag}}$  of the NGSL stars. *Lower panel:* A shifted  $\chi_i T$ , i.e. a  $\chi_i T$  run after a small shifting of the NGSL spectrum.



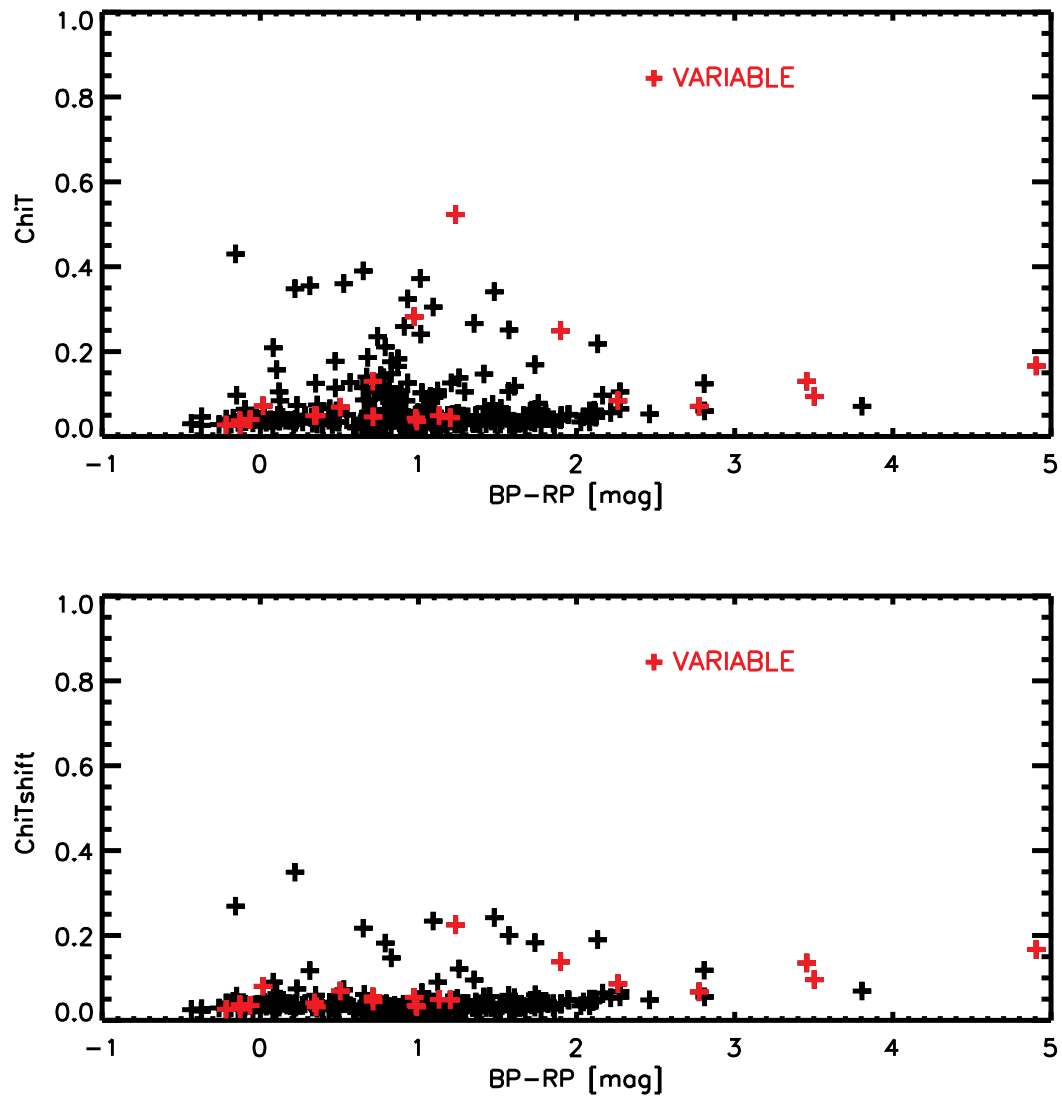


**Fig. 22.** NGSL spectra: *Upper panel:*  $\chi_i T$  versus BP-RP mag of the NGSL stars. *Lower panel:* An adjusted  $\chi_i T$ , i.e. a  $\chi_i T$  run after a small rescaling of the NGSL spectrum.

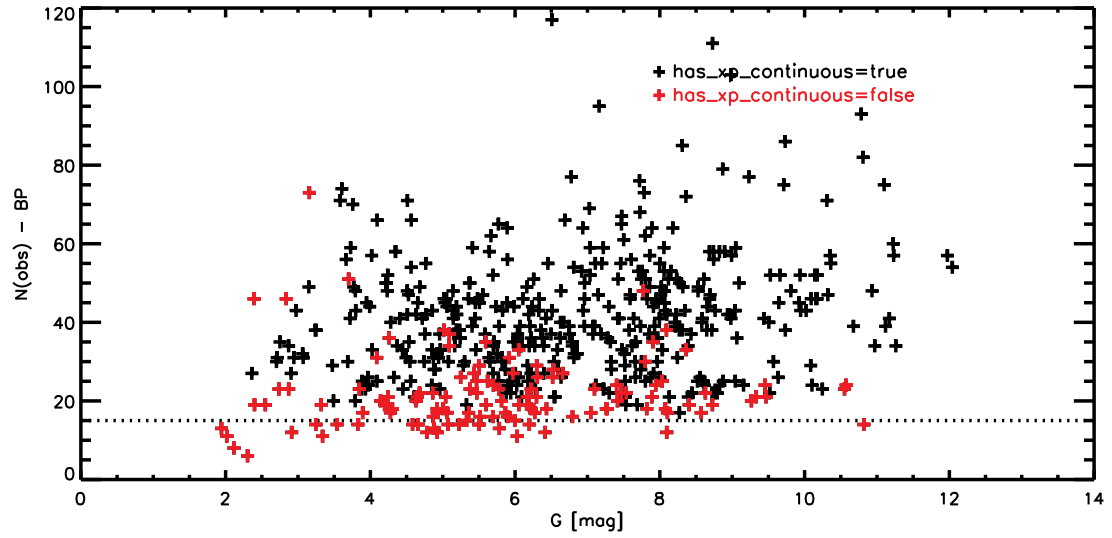


Fig. 23. NGSL spectra: Number of observation in BP-band versus Gmag.

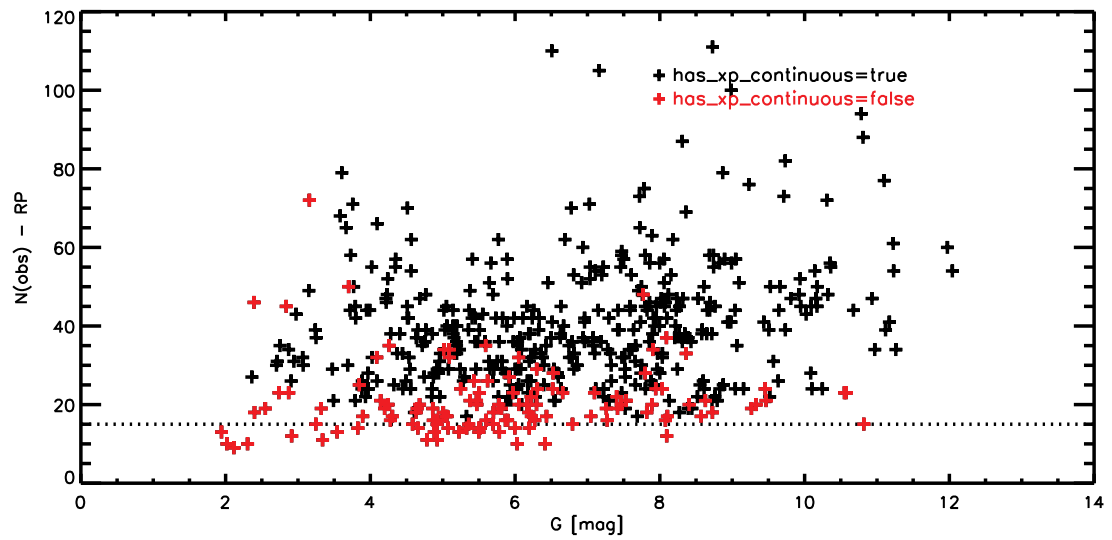


Fig. 24. NGSL spectra: Number of observation in RP-band versus Gmag.

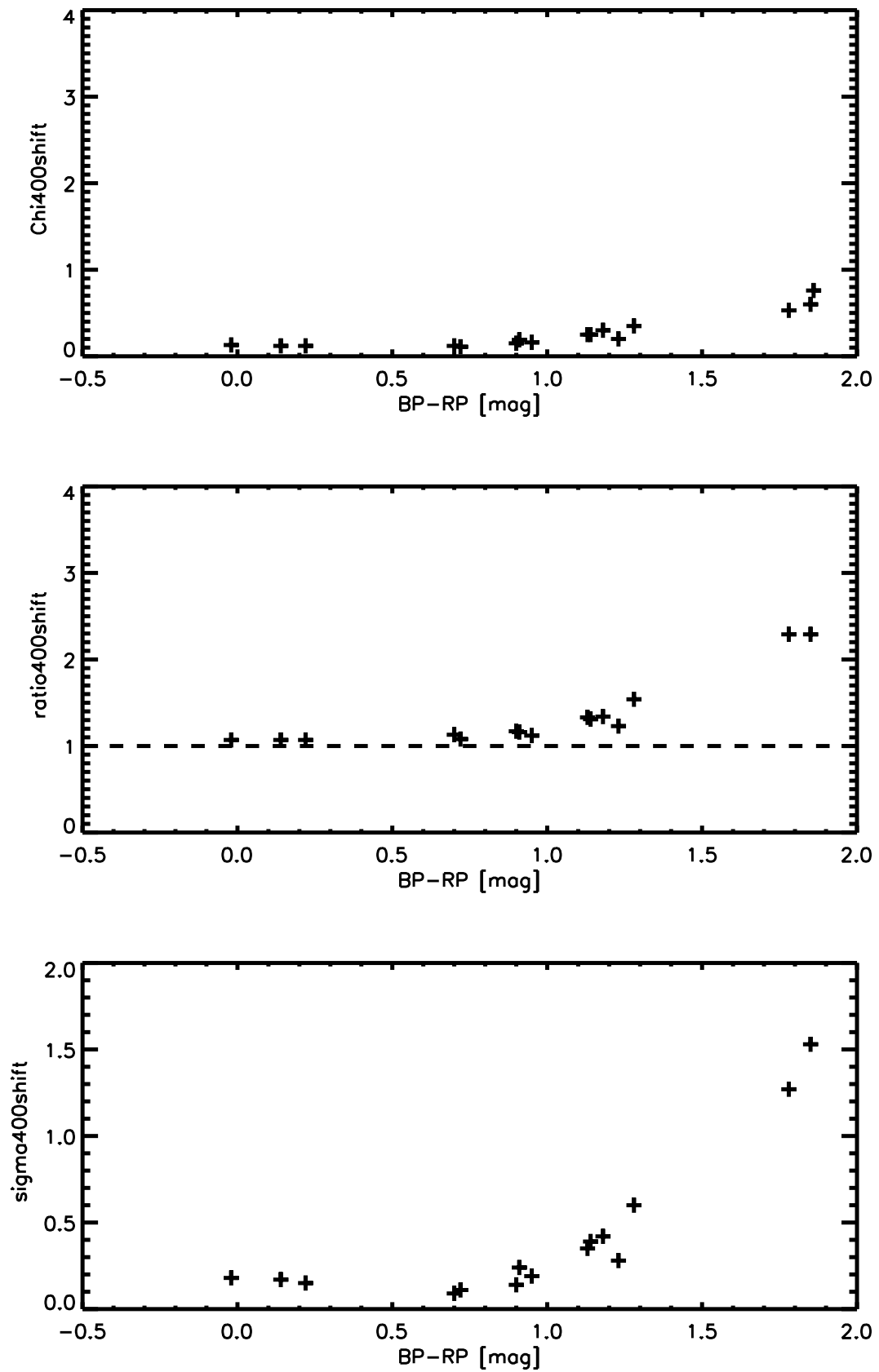


Fig. 25. NGSL spectra: the best sample of NGSL spectra (with the small shift in flux applied). Again the sigma is higher for sources with  $BP-RP > 1$  mag.

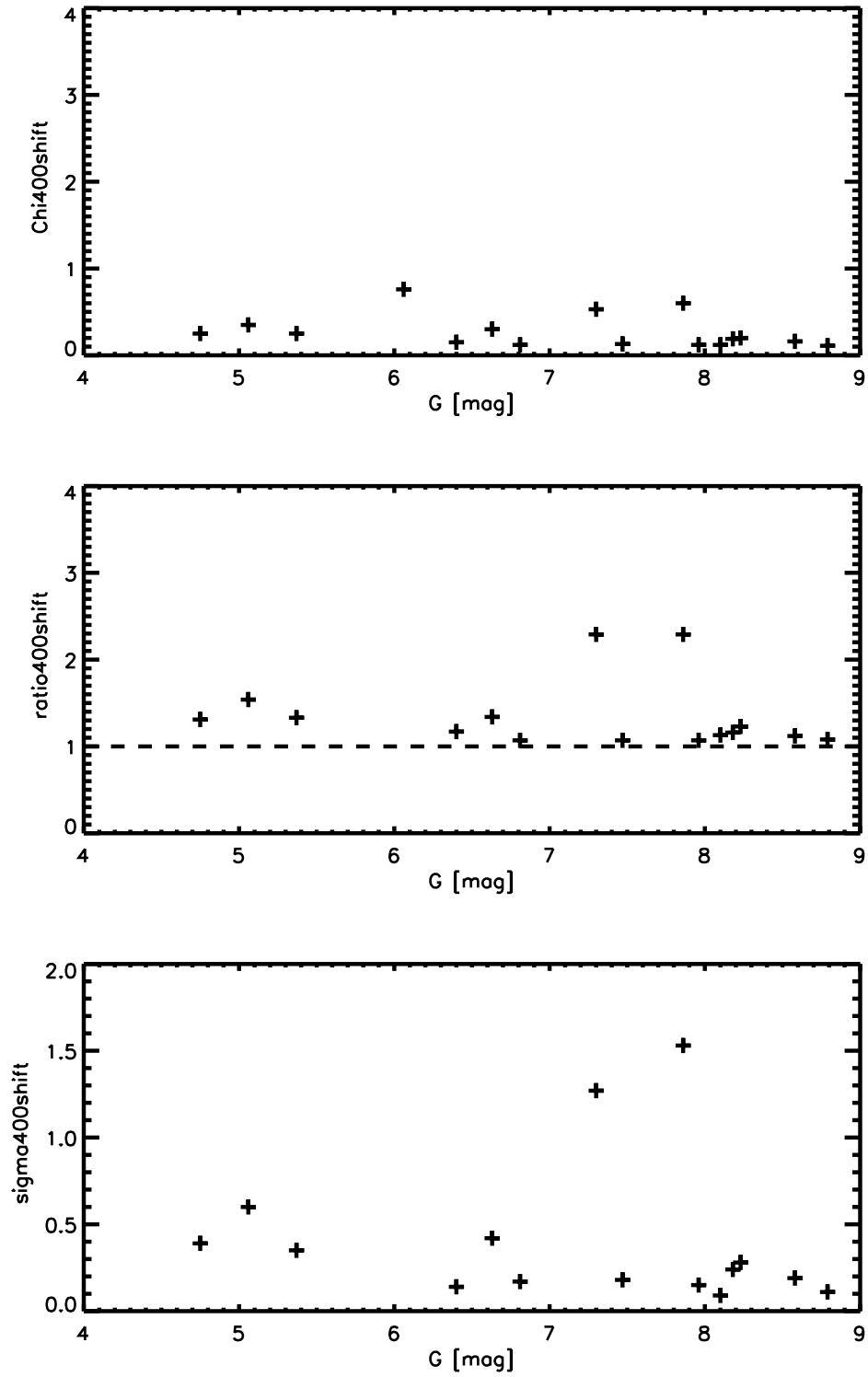


Fig. 26. NGSL spectra: G mag versus fitting parameters below 400 nm (chi, ratio, sigma).

**Table 5.** List of the best 16 NGSL stars (OK and with deviation within 1%).

Gaia ID	XSL	G [mag]	BP-RP [mag]	fact	chi (shift)	chiB (shift)	chiR (shift)	ratioB	sigmaB	ratioR	sigmaR
575775829575361664	HD005256	8.579	0.953	0.991	0.021	0.029	0.013	0.998	0.048	1.008	0.020
4646981136249320832	HD017072	6.395	0.903	0.994	0.022	0.027	0.017	1.007	0.043	1.012	0.023
3316788773511666944	HD040573	7.474	-0.015	0.982	0.038	0.041	0.028	1.004	0.096	1.026	0.063
2889759622882091392	HD041667	8.226	1.230	0.988	0.024	0.041	0.012	0.984	0.052	1.003	0.019
3169175179954291968	HD060319	8.792	0.721	0.999	0.022	0.026	0.017	1.003	0.037	1.006	0.022
5613806071620843392	HD062412	5.367	1.130	0.989	0.026	0.031	0.021	1.010	0.056	1.017	0.029
5300811257630147200	HD074088	6.065	1.860	0.993	0.027	0.044	0.020	1.027	0.113	1.013	0.026
5326028110134118272	HD079349	7.859	1.852	1.000	0.031	0.060	0.019	0.998	0.089	1.005	0.026
5676911545051183872	HD082734	4.753	1.136	0.993	0.029	0.036	0.022	1.003	0.063	1.018	0.032
1127168988075416192	HD086322	6.628	1.180	0.994	0.026	0.033	0.020	1.004	0.062	1.017	0.028
615540938902909440	HD086986	7.964	0.223	0.989	0.031	0.035	0.023	1.000	0.083	1.016	0.049
1491217459831454848	HD126511	8.178	0.909	0.983	0.027	0.032	0.022	1.011	0.057	1.020	0.030
4469871906338470528	HD166991	6.812	0.142	0.979	0.041	0.047	0.027	1.006	0.104	1.025	0.059
4285492327595742080	HD173158	7.300	1.776	0.992	0.027	0.035	0.023	1.023	0.080	1.011	0.036
6858374206854249728	HD196892	8.096	0.703	0.990	0.019	0.021	0.016	1.002	0.032	1.014	0.023
6829361221730142848	HD203638	5.056	1.276	0.997	0.029	0.039	0.022	1.009	0.077	1.014	0.030

## 8 SPSS

The SPSS library comprises 150 spectra (Pancino et al. 2021). Gaia EDR3 matches are provided by the authors.

For the SPSS library, 147 BP/RP spectra were retrieved. shown in this html page.

The SPSS spectra have a wavelength bin of 0.1 nm. The spectra were rebinned to the Gaia low resolution and compared with the Gaia DR3 BP/RP spectra. When selecting those spectra with flux deviations within 1%, 55 spectra are retrieved out of 150. 27 of those 55 stars are flagged as "OK", the remaining as "WD".

It appears that the SPSS library contains 25 stars classified as variables in DR3.

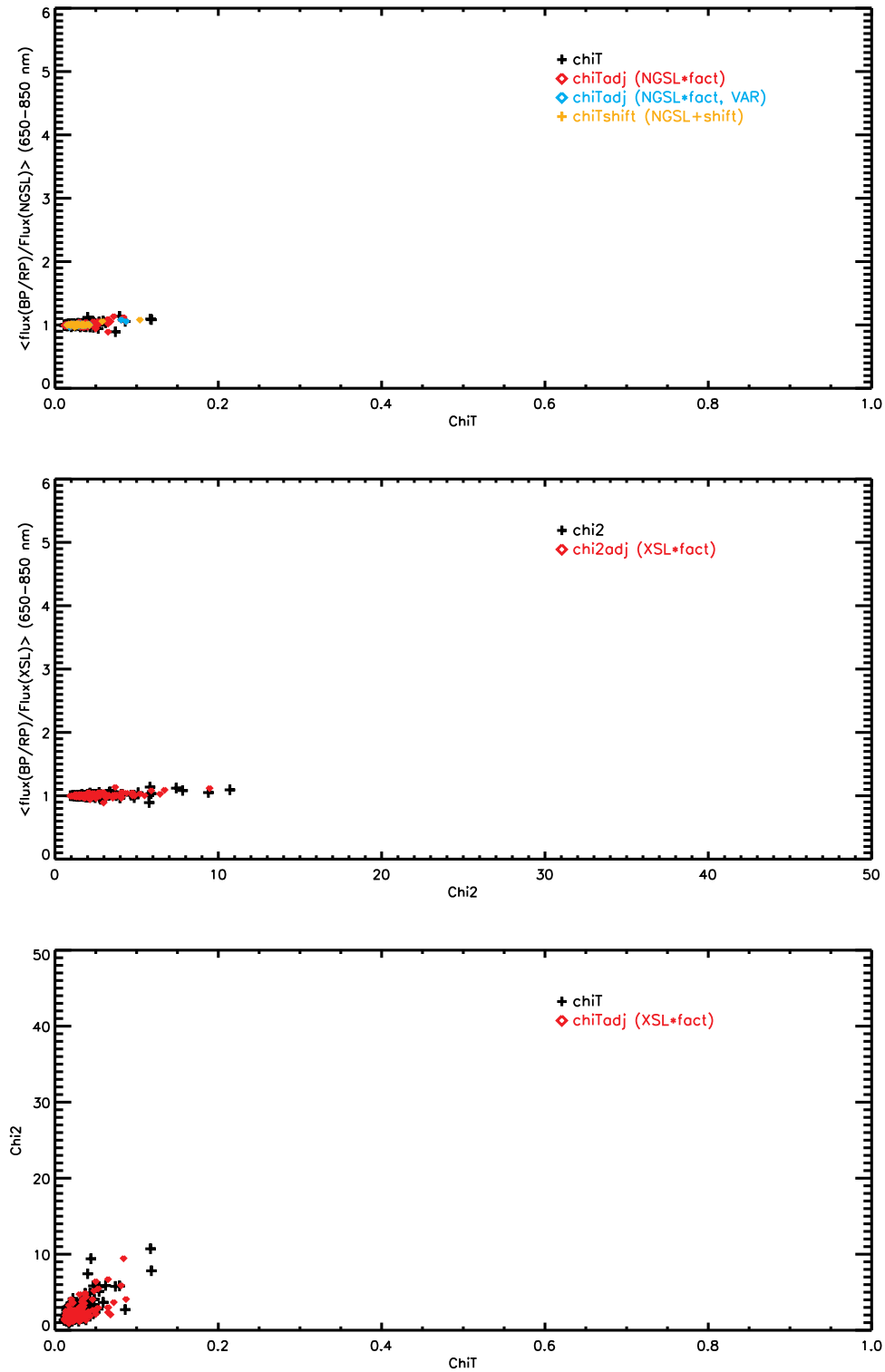


**Fig. 27.** SPSS: the fact value, i.e., the average flux ratio between 650 and 850 nm (BP/RP-SPSS) versus the  $\text{chiT}$  values (black plus signs). A  $\text{chiTadj}$  value is the  $\text{chiT}$  of the modified spectrum  $\text{SPSS} \times \text{fact}$ . A  $\text{chiTshift}$  value is the  $\text{chiT}$  of the modified spectrum  $\text{SPSS} + \text{fact}$ . *Middle panel:* SPSS: the fact value, i.e., the average flux ratio between 700 and 750 nm (BP/RP) versus the  $\text{chi2}$  values (black plus signs). A  $\text{chi2adj}$  value is the  $\text{chi2}$  of the modified spectrum  $\text{SPSS} \times \text{fact}$ . *Lower panel:* SPSS: the  $\text{chiT}$  versus the  $\text{chi2}$  values (black plus signs).

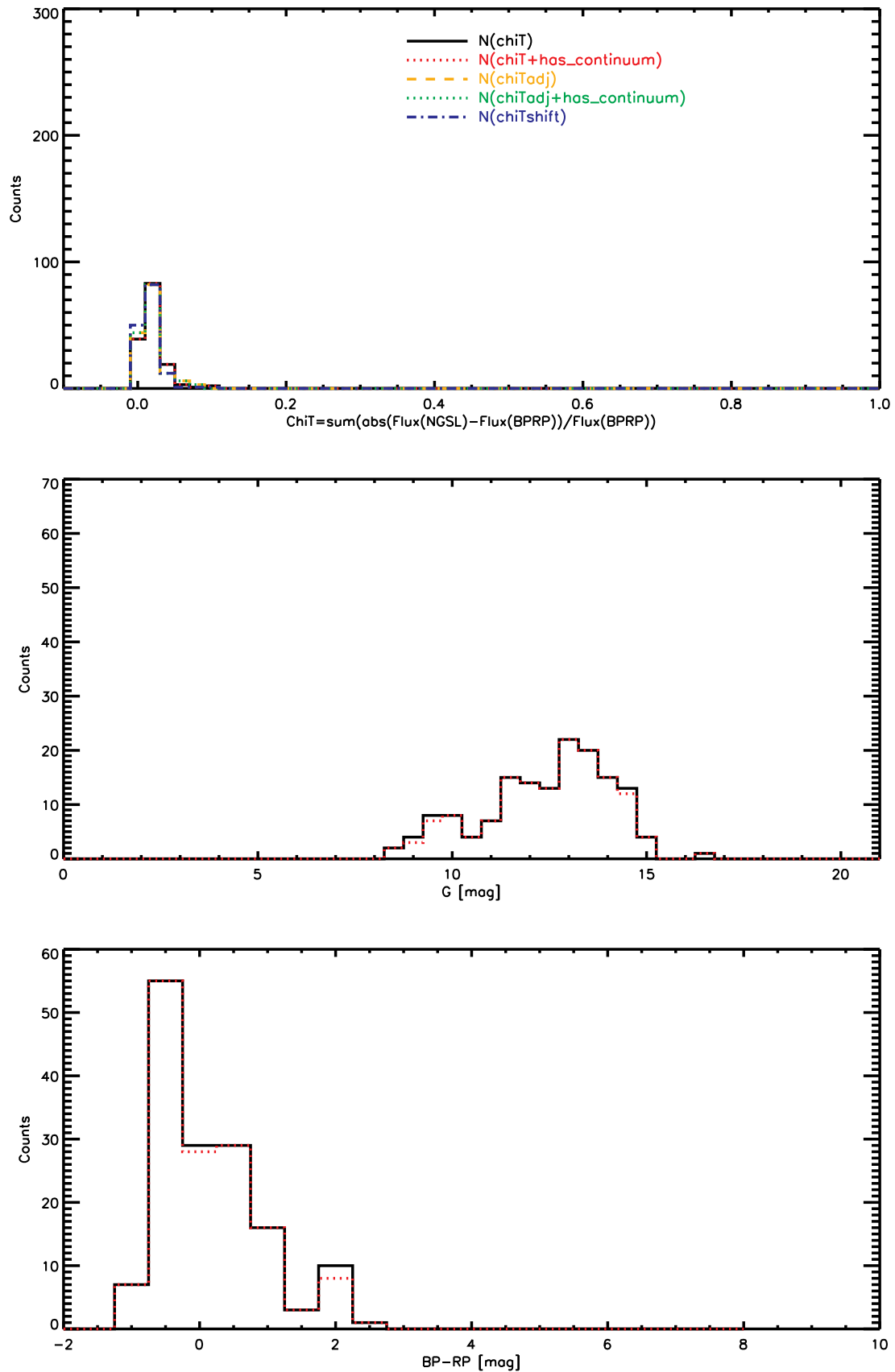


**Fig. 28.** SPSS spectra: *Top panel:* Histogram of the  $\chi T$  parameter. *Middle panel:* Histogram of the G magnitudes. *Lower panel:* Histogram of the BP-RP colors. In red the histograms of those sources with  $\text{has\_xp\_continuous} = \text{'true'}$ .



**Table 6.** SPSS stars classified as VARIABLE by Gaia DR3

id	gaia_id
15	1686708050268594944
24	3126052883671520896
102	572487740053132288
199	2045444369069839744
202	6468623688724871808
270	6462911897617050240
301	2262849634963004416
310	2257815757199848960
326	1564096767011977728
338	1428427236986209024
341	1776317182780536064
7	3304090857318319232
35	1634280312200704768
104	356922880493142016
121	3788194488314248832
124	4019458647338779648
130	3685507214745543040
158	2323394345824851584
208	1848336633214247808
209	2300234782654298624
248	1478363619145920640
271	1793946026371051648
304	3406506723313874688
308	3806885288337214848
334	3943234217765374336

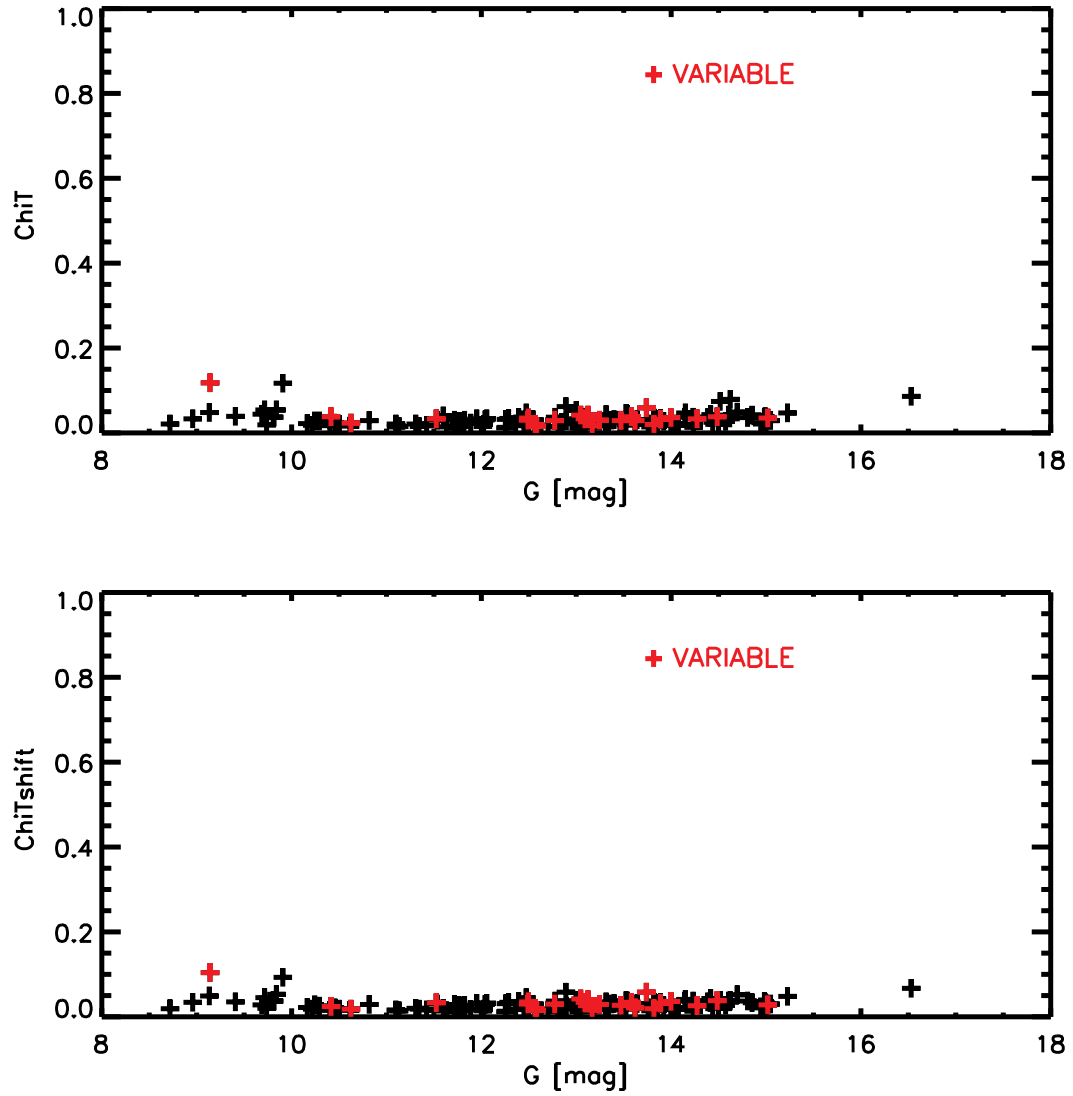


**Fig. 29.** SPSS spectra: *Upper panel:*  $\chi_i T$  versus Gmag of the SPSS stars. *Lower panel:* A shifted  $\chi_i T$ , i.e. a  $\chi_i T$  run after a small shifting of the SPSS spectrum.

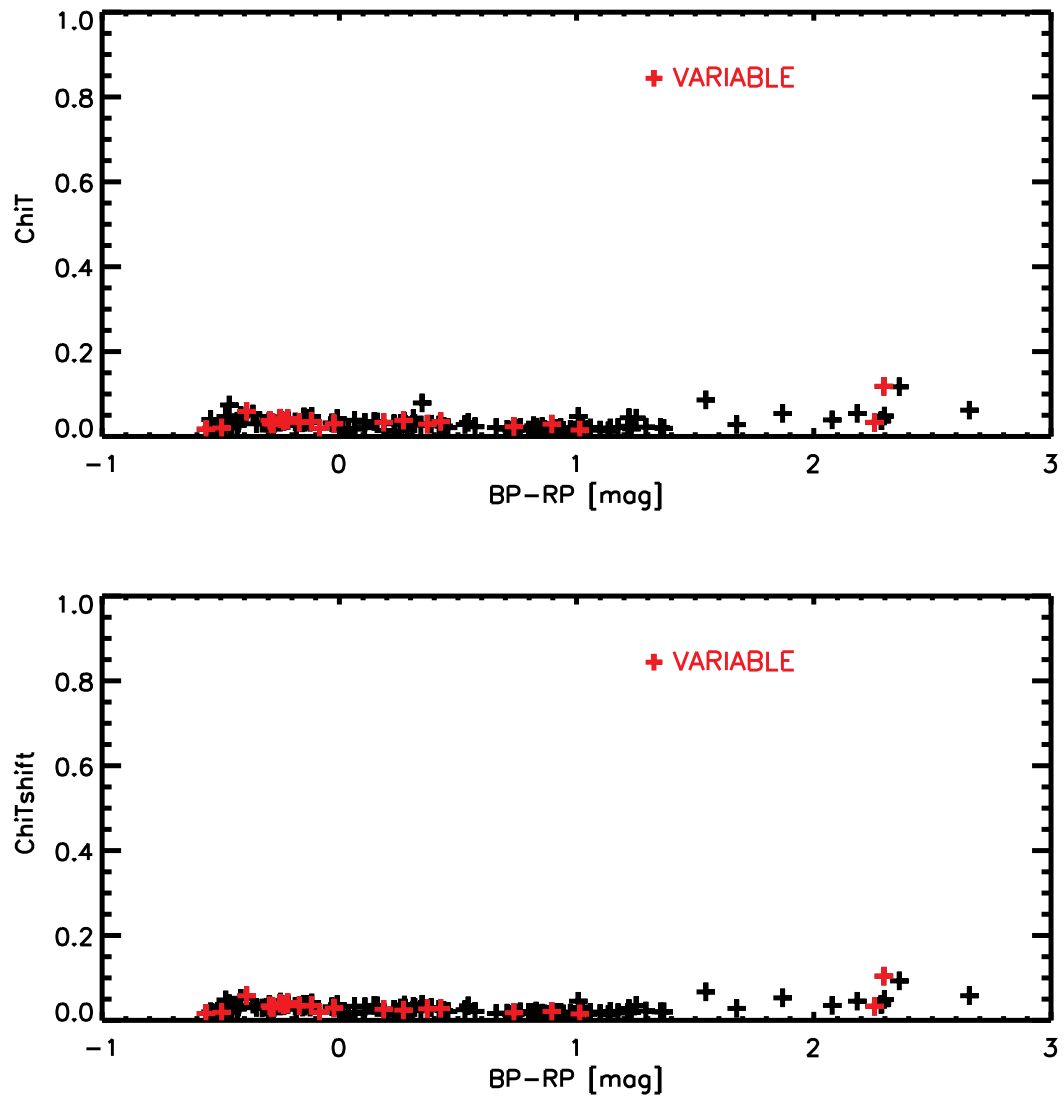


**Fig. 30.** SPSS spectra: *Upper panel:*  $\chi_i T$  versus BP-RP mag of the SPSS stars. *Lower panel:* An adjusted  $\chi_i T$ , i.e. a  $\chi_i T$  run after a small rescaling of the SPSS spectrum.

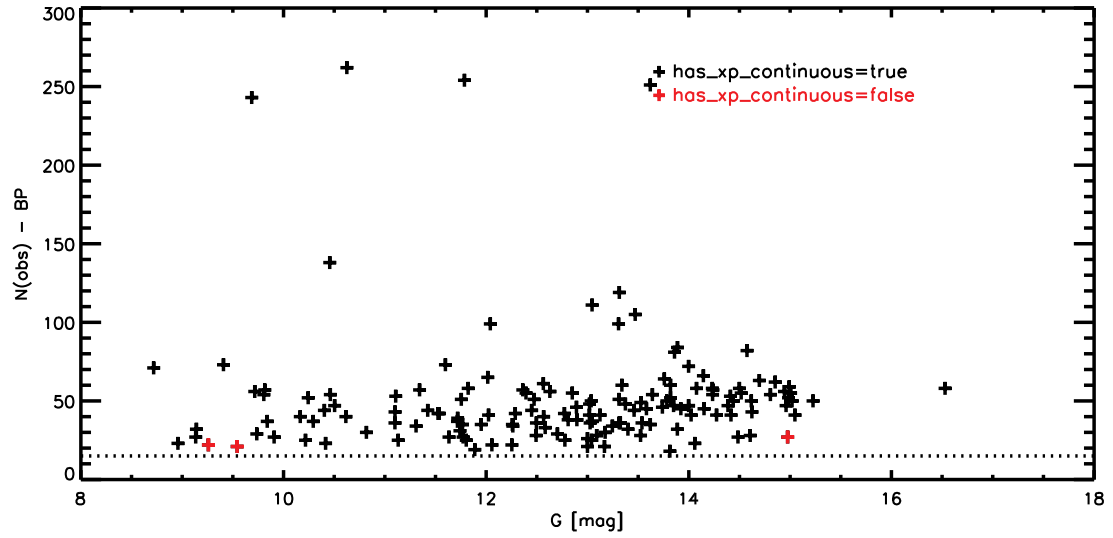


Fig. 31. SPSS spectra: Number of observation in BP-band versus Gmag.

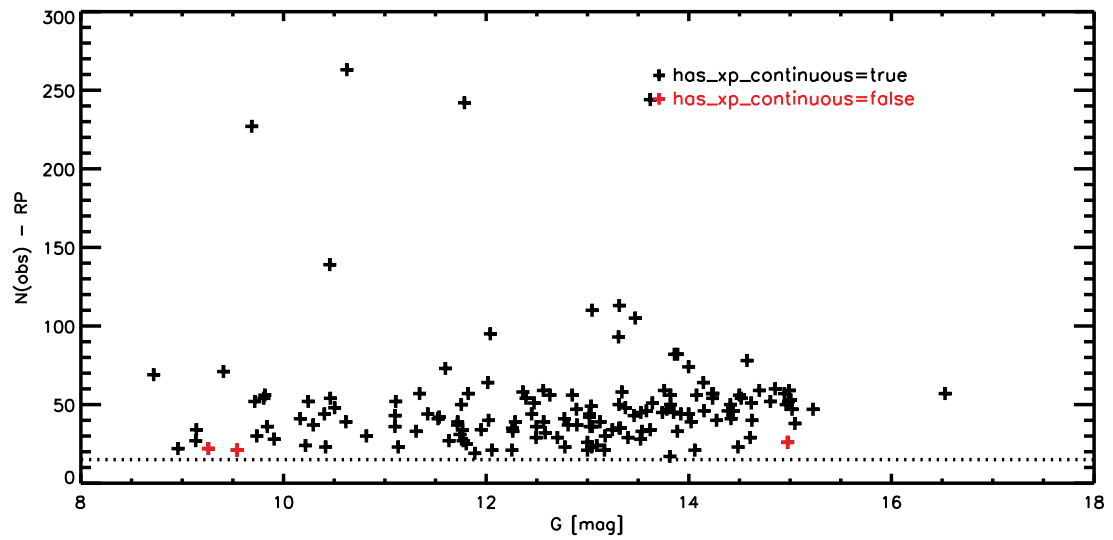
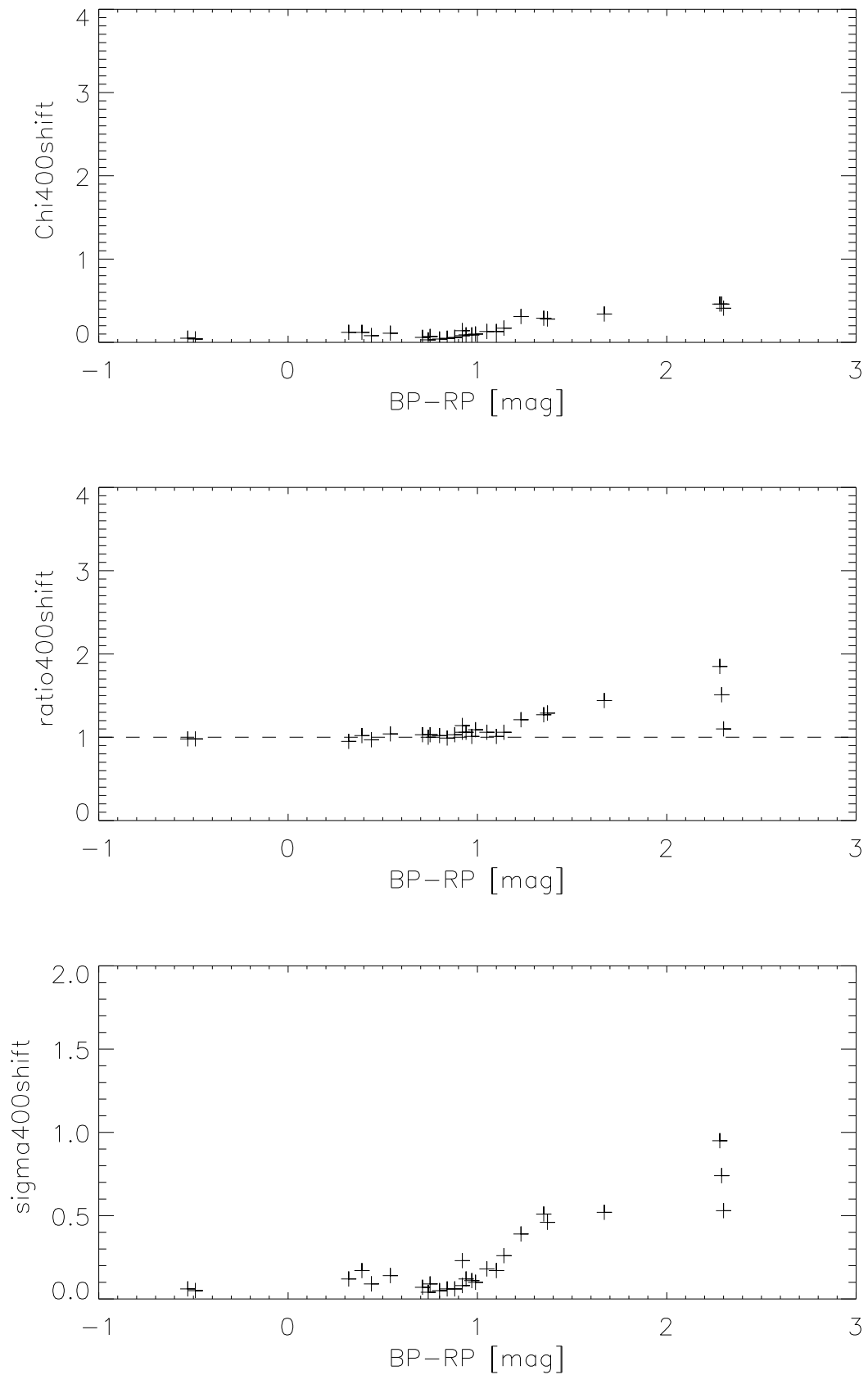
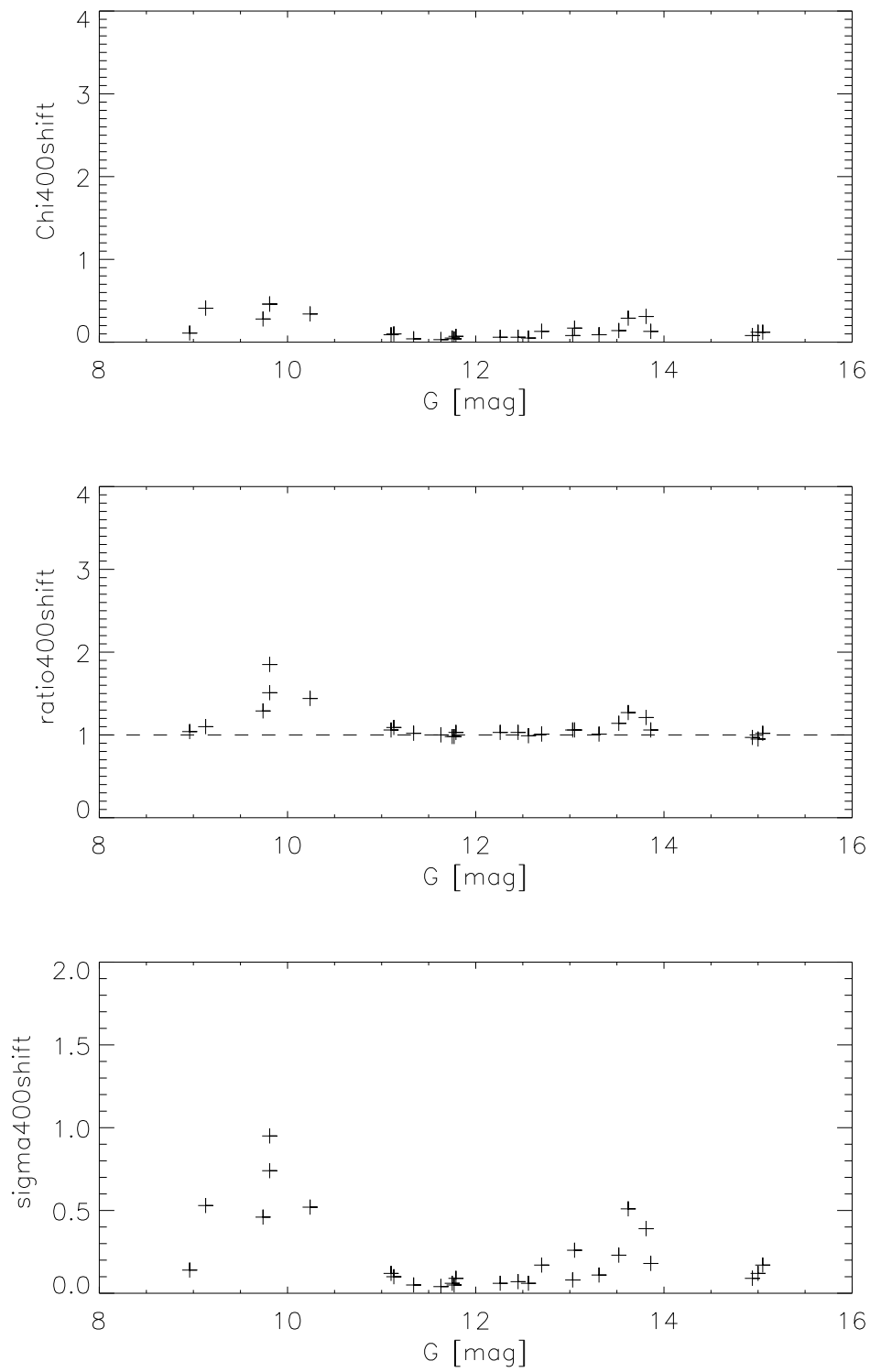


Fig. 32. SPSS spectra: Number of observation in RP-band versus Gmag.



**Fig. 33.** SPSS spectra: the best sample of SPSS spectra (with the small shift in flux applied). Again the sigma is higher for sources with  $BP - RP > 1$  mag.



**Fig. 34.** SPSS spectra:  $G$  mag versus fitting parameters below 400 nm (chi, ratio, sigma).

**Table 7.** List of the best 27 SPSS stars (OK and with deviation within 1%).

Gaia ID	XSL	G [mag]	BP-RP [mag]	fact	chi (shift)	chiB (shift)	chiR (shift)	ratioB	sigmaB	ratioR	sigmaR
3853478472249151616	116	12.263	0.879	0.998	0.013	0.014	0.013	1.006	0.018	1.006	0.018
3817965105665685504	122	11.131	0.990	1.004	0.014	0.016	0.013	1.004	0.024	1.004	0.020
2541942588451597440	323	15.005	0.318	0.999	0.030	0.030	0.030	1.001	0.062	1.010	0.046
3348071528591318272	351	13.524	0.918	0.998	0.019	0.022	0.016	1.002	0.032	1.005	0.025
2633603478379307904	23	11.773	-0.489	1.003	0.018	0.018	0.016	1.000	0.022	1.000	0.034
3935488605023787392	27	11.755	-0.534	1.008	0.017	0.017	0.018	1.000	0.021	0.987	0.030
4416639085227405952	32	8.958	0.543	1.007	0.034	0.040	0.024	0.981	0.048	1.000	0.035
6210089815971933056	33	11.633	0.741	0.998	0.014	0.013	0.015	1.006	0.018	1.012	0.024
5024640977840398848	39	11.343	0.797	0.980	0.018	0.018	0.018	1.016	0.018	1.017	0.022
1633294634388508416	45	13.045	1.142	0.995	0.021	0.028	0.015	1.005	0.047	1.004	0.020
1633376204407124352	47	13.620	1.354	1.007	0.020	0.030	0.014	0.991	0.050	1.003	0.021
318506871931567616	103	12.703	1.099	1.000	0.016	0.022	0.010	1.013	0.033	1.002	0.016
3520997013687539712	129	9.736	1.368	1.010	0.020	0.032	0.012	0.989	0.046	0.995	0.016
1639946061258413312	133	12.564	0.841	0.990	0.015	0.014	0.016	1.004	0.019	1.012	0.025
1406378695954996352	136	11.100	0.944	1.011	0.015	0.018	0.012	0.988	0.019	0.996	0.018
268550015665098880	171	13.025	0.923	0.995	0.012	0.014	0.009	1.007	0.018	1.002	0.014
1272306378368710528	191	13.307	0.974	1.003	0.017	0.018	0.016	0.994	0.026	1.006	0.025
4524670913035545344	259	13.859	1.048	1.001	0.015	0.018	0.013	1.002	0.036	1.005	0.018
4421525074384092032	313	13.813	1.231	0.996	0.019	0.024	0.015	0.997	0.039	1.008	0.021
3683915053189161728	315	12.449	0.707	1.006	0.017	0.019	0.014	1.004	0.028	1.003	0.021
845789153480087936	320	14.944	0.440	1.007	0.023	0.024	0.023	1.003	0.043	0.996	0.034
3277270538903180160	328	10.243	1.675	1.007	0.028	0.059	0.014	0.978	0.083	0.997	0.020
3089711447388931584	332	9.133	2.298	1.026	0.049	0.115	0.033	0.928	0.139	0.985	0.047
4519789321942643072	339	9.815	2.283	1.004	0.037	0.096	0.022	0.989	0.134	1.000	0.029
4519789081415296128	340	9.805	2.287	1.007	0.038	0.098	0.023	0.977	0.139	0.997	0.029
4227837442496206592	343	15.047	0.387	0.997	0.030	0.033	0.023	1.009	0.063	1.005	0.038
5284204302730217984	348	11.786	0.753	1.004	0.017	0.018	0.017	1.004	0.023	0.995	0.023

## 9 CALSPEC library

The CALSPEC library comprises 121 stars, which are flux standards on the HST system. The composite spectra were acquired with the Hubble telescope.

101 are the matches with Gaia DR3 BP/RP spectra. When checking on SIMBAD, 25 WD are identified and 65 normal stars (no variables, no emission lines). Only 33 of the normal 65 stars have CALSPEC spectra with flux densities within 1% of those in BP/RP from DR3 and their G-magnitudes range from 6 to 13 mag.

Figures 35, 36, 37, 38, 39, 40, 41, and 42 display histograms of the G-mag and BP-RP colors and chiT values of stars in the CALSPEC library.

### 9.1 CALSPEC and PVL

The PVL by Elena Pancino contains 62 stars and 44 of those are marked as CALSPEC. The PVL is made of stars with spectra of good quality (NGSL or CALSPEC) and not included in the SPSS library. 43 of the 44 PVL/CALSPEC spectra are in the CALSPEC full-coverage list.

The CALSPEC library has been revised and extended with currently 121 spectra with full coverage (Bohlin & Lockwood 2022). A number of CALSPEC stars (79) were not listed at the time of the PVL compilation. 23 of these 79 stars are non-variable, single, simbad=OK, and have a Gaia DR3 BPRP spectrum (15 new stars and 8 stars in overlap with the SPSS library).

### 9.2 Comparison: 44 stars CALSPEC and PVL

### 9.3 Comparison: 8 stars CALSPEC and SPSS



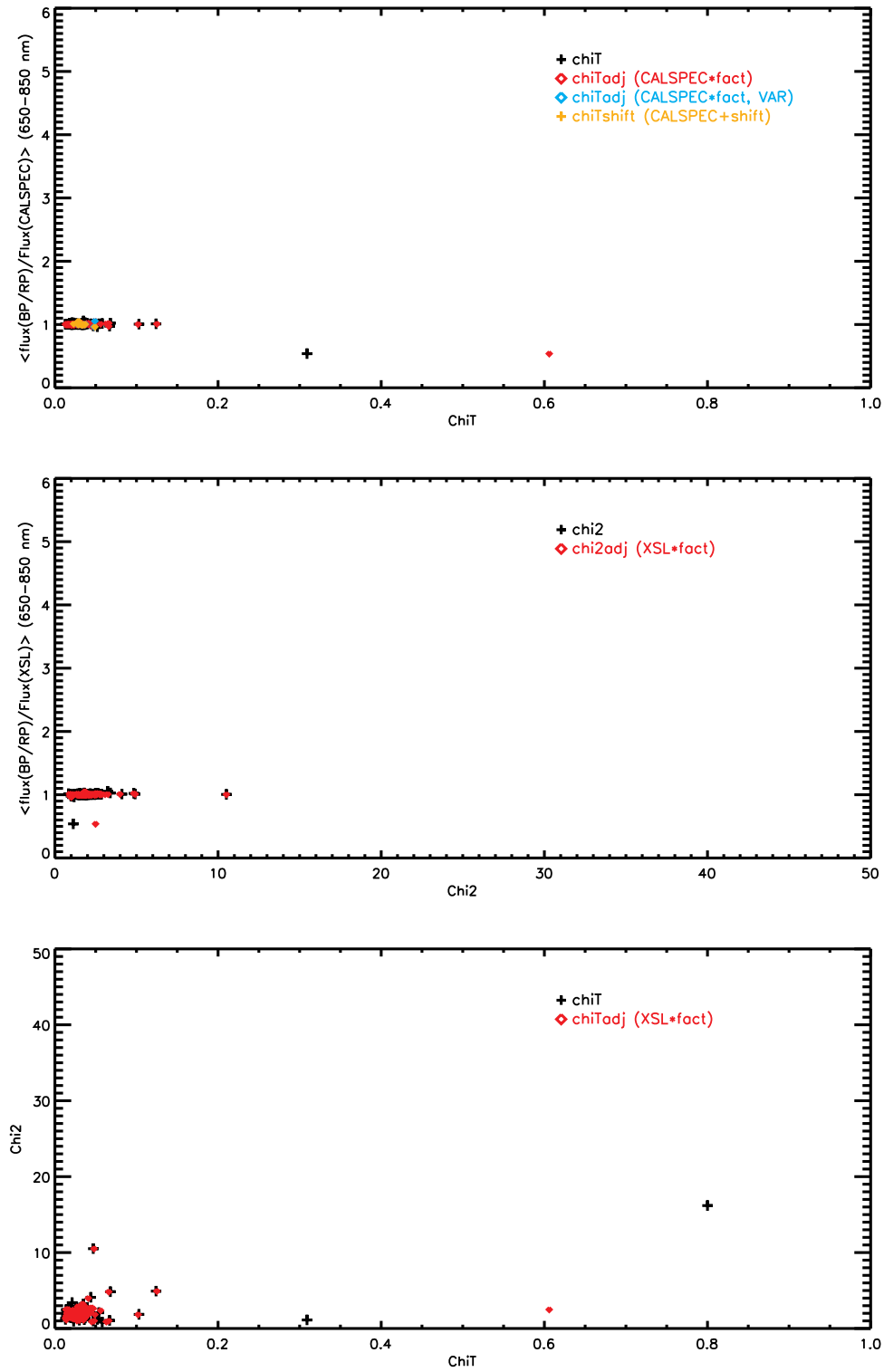


**Fig. 35.** CALSPEC: the fact value, i.e., the average flux ratio between 650 and 850 nm (BP/RP-CALSPEC) versus the  $\chi^2$  values (black plus signs). A  $\chi^2_{\text{adj}}$  value is the  $\chi^2$  of the modified spectrum  $\text{CALSPEC} \times \text{fact}$ . A  $\chi^2_{\text{shift}}$  value is the  $\chi^2$  of the modified spectrum  $\text{CALSPEC} + \text{fact}$ . *Middle panel:* CALSPEC: the fact value, i.e., the average flux ratio between 700 and 750 nm (BP/RP) versus the  $\chi^2$  values (black plus signs). *Lower panel:* CALSPEC: the  $\chi^2$  versus the  $\chi^2$  values (black plus signs).

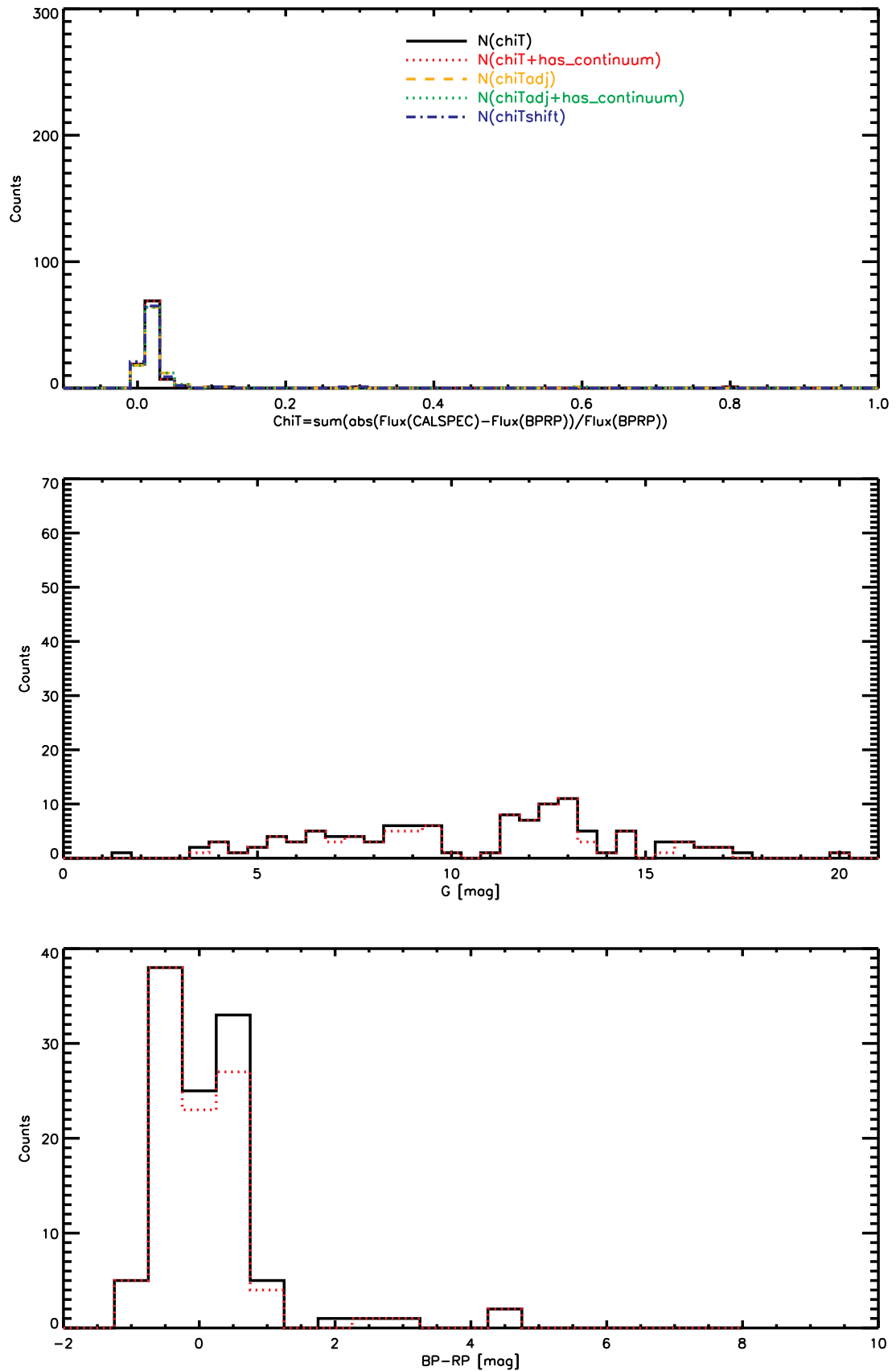


**Fig. 36.** CALSPEC spectra: *Top panel:* Histogram of the  $\chi T$  parameter. *Middle panel:* Histogram of the G magnitudes. *Lower panel:* Histogram of the BP-RP colors. In red the histograms of those sources with `has_xp_continuous='true'`.

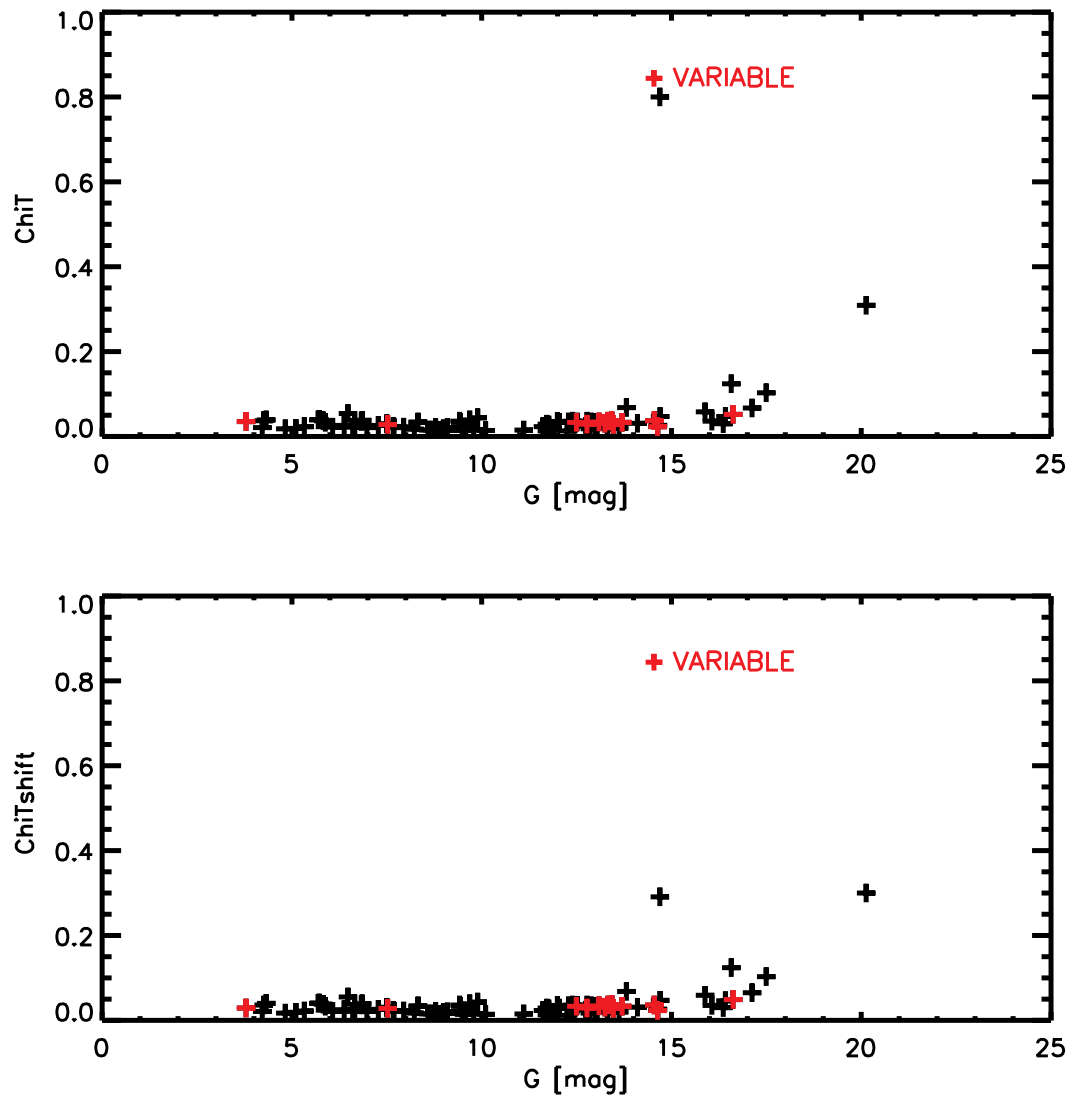


**Fig. 37.** CALSPEC spectra: *Upper panel:*  $\chi_i T$  versus  $G_{\text{mag}}$  of the CALSPEC stars. *Lower panel:* A shifted  $\chi_i T$ , i.e. a  $\chi_i T$  run after a small shifting of the CALSPEC spectrum.

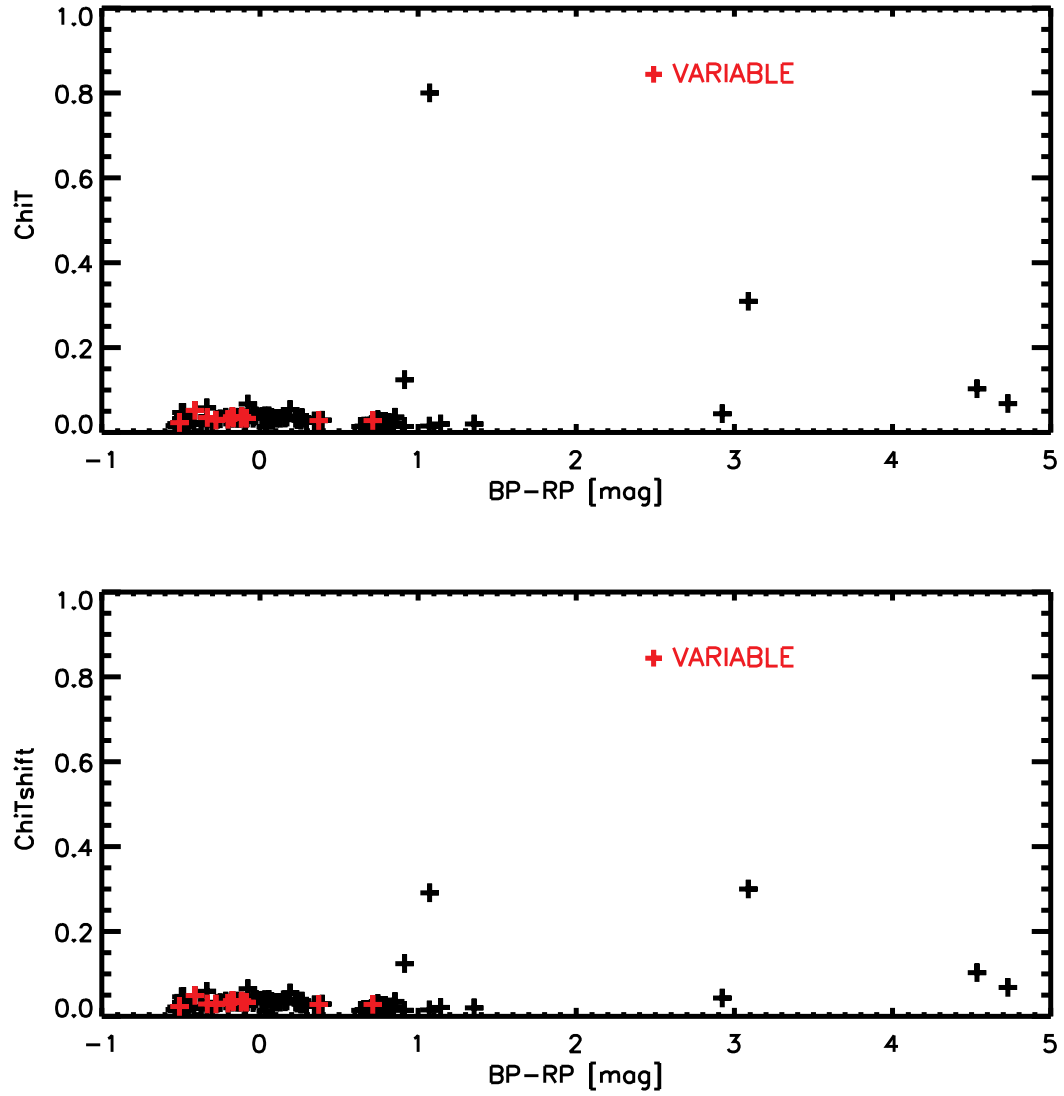


**Fig. 38.** CALSPEC spectra: *Upper panel:*  $\chi T$  versus BP-RP mag of the CALSPEC stars. *Lower panel:* An adjusted  $\chi T$ , i.e. a  $\chi T$  run after a small rescaling of the CALSPEC spectrum.

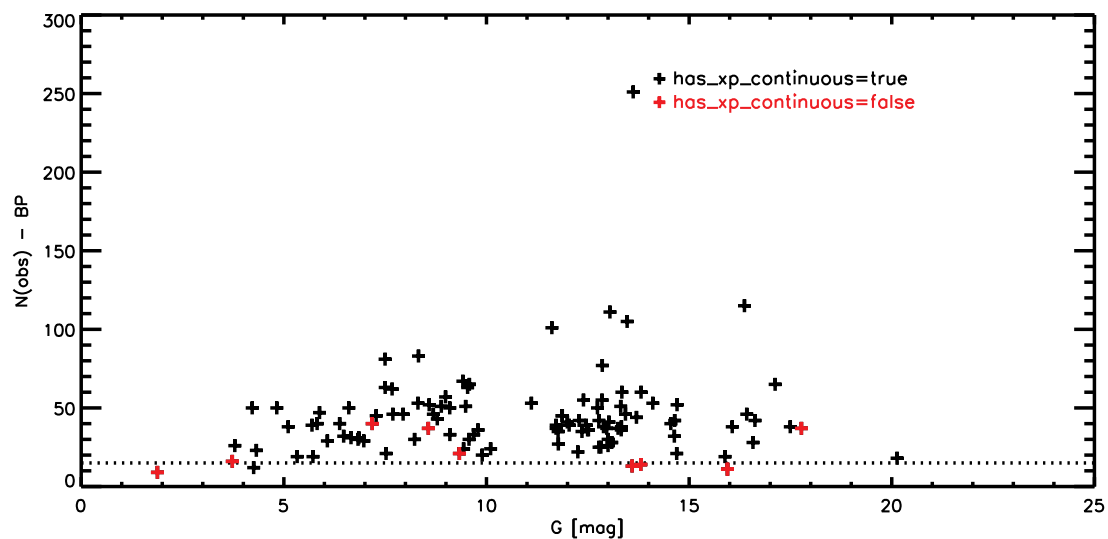


Fig. 39. CALSPEC spectra: Number of observation in BP-band versus Gmag.

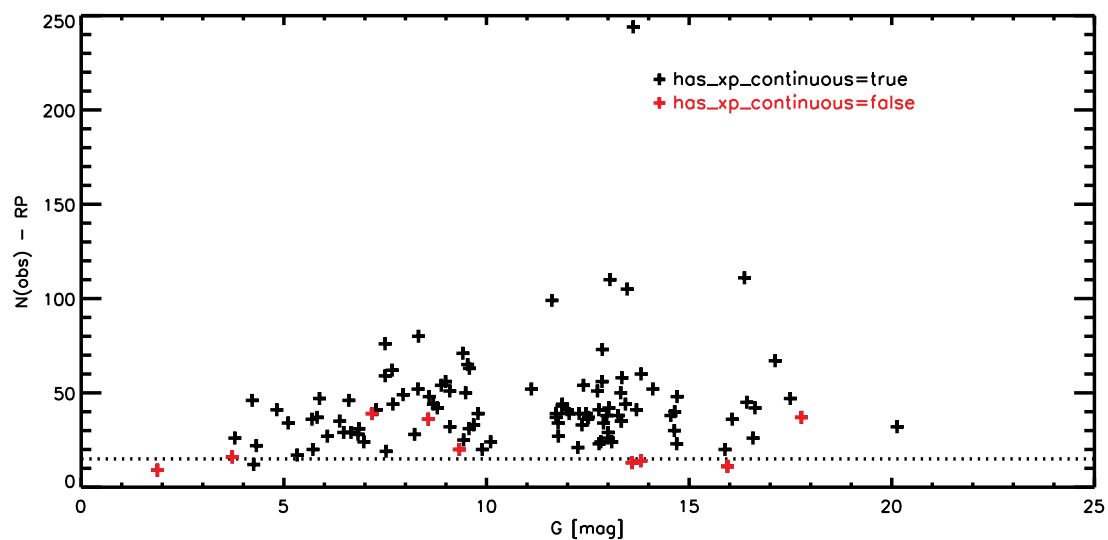
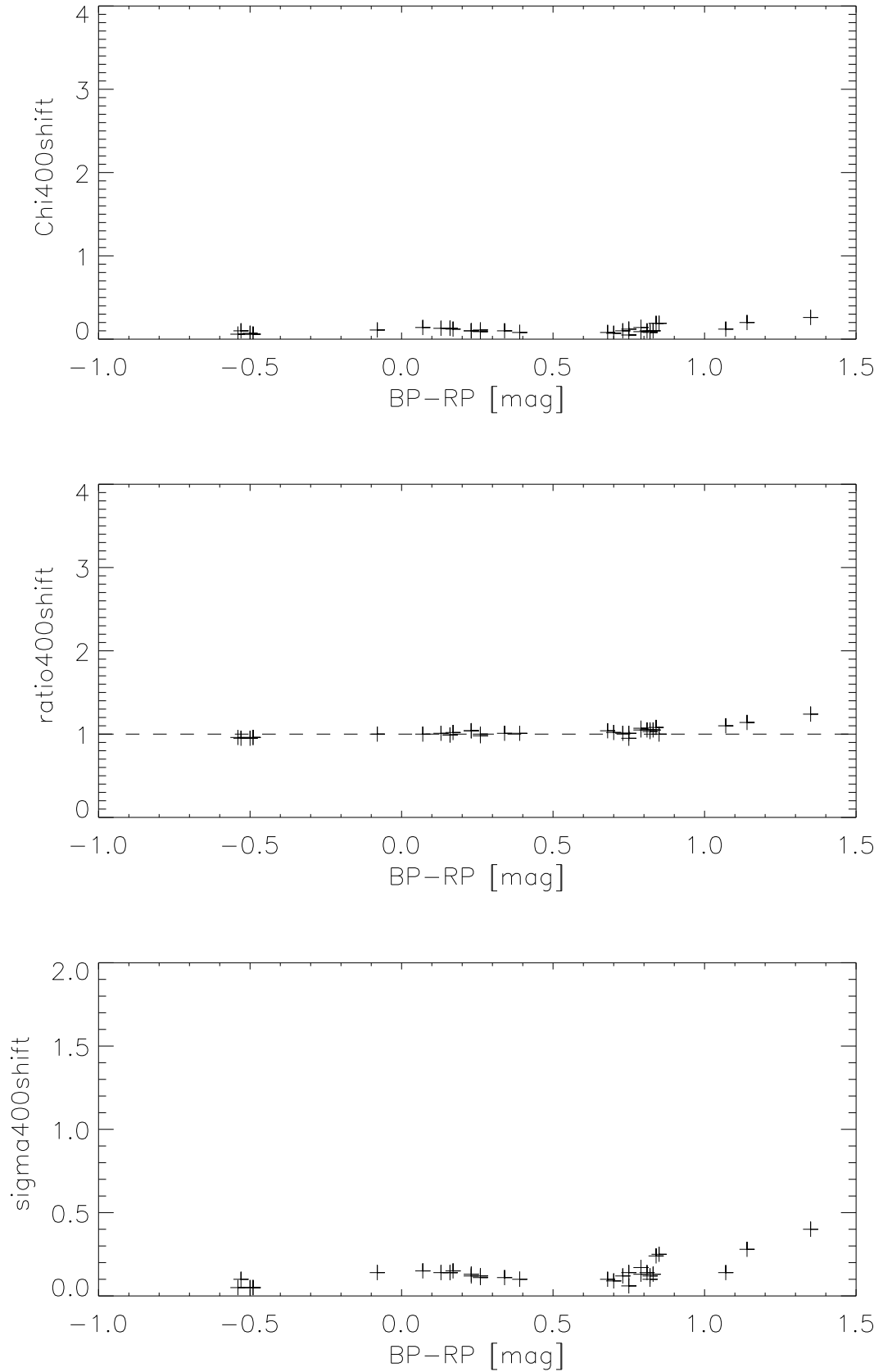
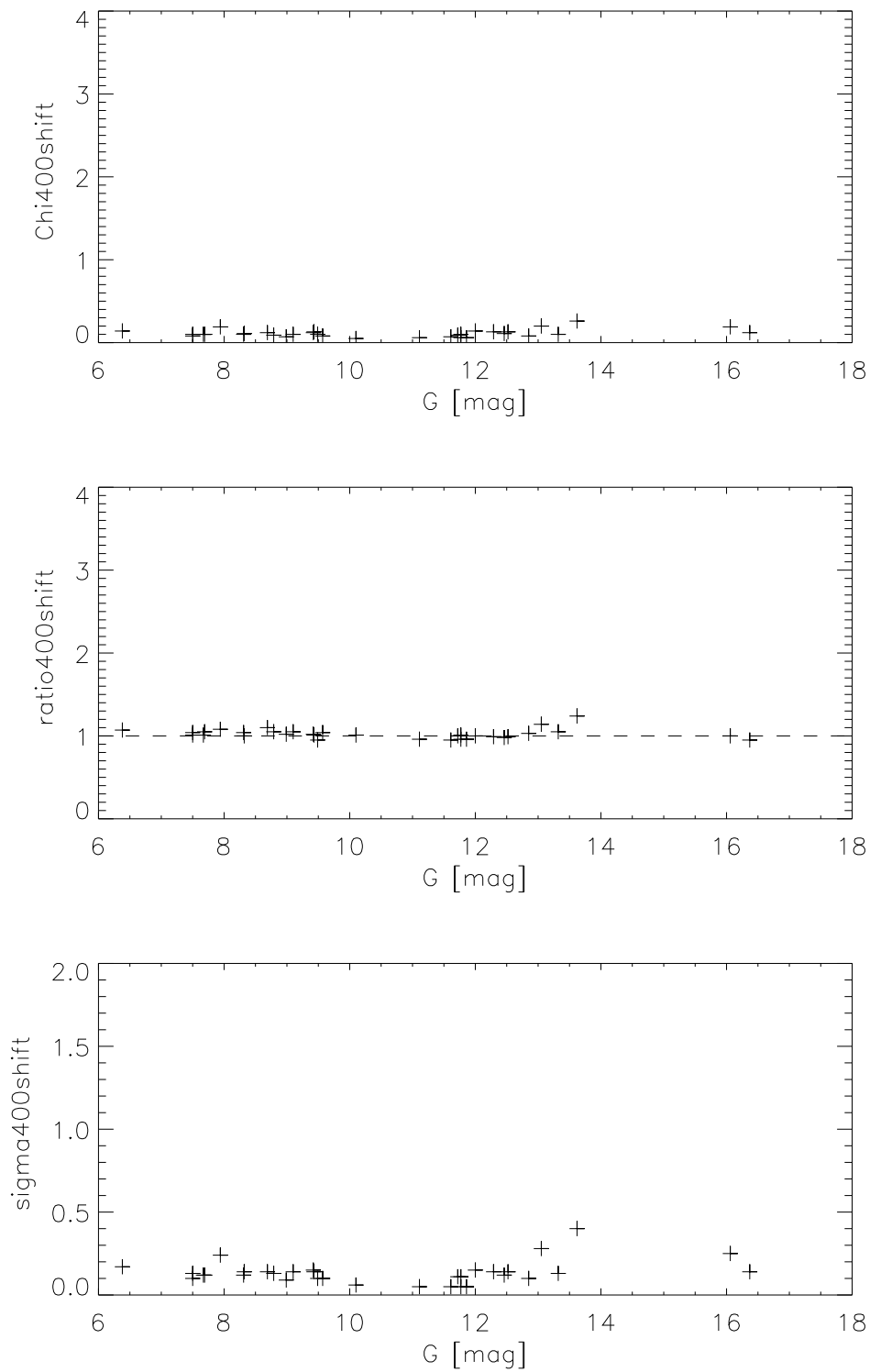


Fig. 40. CALSPEC spectra: Number of observation in RP-band versus Gmag.



**Fig. 41.** CALSPEC spectra: the best sample of CALSPEC spectra (with the small shift in flux applied). Again the sigma is higher for sources with  $BP-RP > 1$  mag.



**Fig. 42.** CALSPEC spectra: G mag versus fitting parameters below 400 nm (chi, ratio, sigma).

**Table 8.** List of the best 33 CALSPEC stars (OK and with deviation within 1%).

Gaia ID	XSL	G [mag]	BP-RP [mag]	fact	chi (shift)	chiB (shift)	chiR (shift)	ratioB	sigmaB	ratioR	s
1651137131123978112	1732526	12.515	0.157	1.003	0.035	0.040	0.023	0.998	0.091	1.002	
1633143932573832448	17403462	12.461	0.260	0.999	0.029	0.033	0.020	1.002	0.078	1.006	
1633585107317144960	2MASSJ17571324+67034	11.767	0.344	0.999	0.027	0.030	0.020	1.003	0.067	1.002	
2158745262705810304	2MASSJ18022716+60433	11.996	0.074	1.005	0.035	0.040	0.024	1.003	0.095	1.001	
2161093682102883712	1805292	12.287	0.159	1.008	0.034	0.038	0.025	1.002	0.093	1.000	
2160839724980689408	1812095	11.717	0.258	1.001	0.029	0.034	0.019	1.002	0.081	1.003	
1144974578159253632	AGK+81_266	11.860	-0.539	1.005	0.016	0.016	0.015	0.997	0.022	0.997	
731253779217024640	BD+29_2091	10.102	0.749	1.003	0.014	0.019	0.008	0.990	0.023	0.998	
1032197606073957888	BD+54_1216	9.569	0.679	1.002	0.016	0.021	0.009	0.997	0.029	1.001	
1135587497636732672	BD+75_325	9.485	-0.528	1.005	0.022	0.023	0.017	0.989	0.027	0.997	
5057499161282786432	C26202	16.366	0.745	1.001	0.030	0.028	0.031	0.987	0.035	0.999	
2633603478379307904	FEIGE110	11.773	-0.489	1.008	0.020	0.021	0.015	0.999	0.030	0.991	
781164326766404736	FEIGE34	11.107	-0.489	1.006	0.015	0.016	0.012	0.995	0.021	1.001	
5040300909638155520	HD009051	8.688	1.071	1.006	0.015	0.022	0.010	0.998	0.037	0.997	
4881345510044485120	HD031128	8.990	0.704	1.007	0.018	0.024	0.010	0.996	0.031	0.997	
5384905720847544192	HD101452	7.497	0.394	1.002	0.029	0.036	0.016	0.993	0.065	1.004	
6182594053814895872	HD115169	9.097	0.811	0.998	0.020	0.027	0.013	0.997	0.041	0.997	
1550544530286455680	HD116405	8.322	-0.080	1.006	0.034	0.038	0.023	0.999	0.087	1.000	
1335880415564253312	HD159222	6.377	0.793	1.009	0.025	0.036	0.012	0.999	0.056	0.997	
6634011506225360640	HD167060	8.786	0.792	0.999	0.021	0.024	0.016	0.996	0.036	0.995	
2254144423451326080	HD180609	9.416	0.171	1.005	0.036	0.043	0.021	0.999	0.094	0.999	
6342346358822630400	HD185975	7.942	0.845	1.003	0.022	0.032	0.011	0.997	0.047	0.997	
4992412432308644224	HD2811	7.500	0.235	1.006	0.031	0.036	0.021	0.995	0.076	1.003	
3444212584803426048	HD37725	8.309	0.225	1.008	0.033	0.039	0.021	0.999	0.086	1.000	
2902205991429301888	HD37962	7.690	0.815	1.010	0.021	0.029	0.012	0.988	0.039	0.997	
2915523482424724224	HD38949	7.672	0.734	1.001	0.023	0.029	0.015	0.990	0.036	1.004	
3167212139383161216	HD55677	9.435	0.128	1.005	0.033	0.037	0.024	1.000	0.090	0.997	
1473687671071803520	HZ44	11.613	-0.501	1.000	0.023	0.026	0.013	0.997	0.032	1.005	
1633376204407124352	2MASSJ17583798+66465	13.620	1.354	1.001	0.020	0.031	0.012	0.994	0.051	1.003	
1633294634388508416	KF08T3	13.045	1.142	0.998	0.021	0.029	0.014	1.004	0.046	0.999	
1399559249961569792	P177D	13.324	0.829	1.004	0.019	0.022	0.016	0.999	0.034	1.004	
1312054926303736704	P330E	12.850	0.819	1.003	0.017	0.021	0.013	0.999	0.032	1.002	
1429541695100150656	SNAP-2	16.064	0.854	0.996	0.035	0.032	0.039	0.988	0.043	1.010	



## 10 STELIB library

The list of 255 stars of the STELIB library was obtained from the Vizier database. The spectra were acquired with the 1 m Jacobus Kaptein Telescope in La Palma and with the 2.3 m of the Australian National University at Siding String (Le Borgne et al. 2003). The spectra were obtained by combined observations with several gratings to cover from 320 to 950 nm. The original spectral resolution was  $< 0.3$  nm and the distributed spectra have a bin of 0.1 nm.

243 of these stars have a Gaia DR3 source\_id and 179 have a Gaia DR3 BP/RP spectra. By retaining only STELIB spectra with a full coverage and with a Gaia DR3 BP/RP match, 78 spectra remain. Unfortunately, after a search on SIMBAD to exclude variable and binaries, only 34 stars are left. Furthermore, by imposing that the average of the residuals (differences of the STELIB spectra and Gaia DR3 BP/RP spectra) is in average within 1%, only 3 spectra remain (HD075732, HD079452, and HD081192).

## 11 Summary of the analyzed libraries

The content of this report is illustrated in the webpage <https://lamortadella.github.io/BPRPLibraries/index.html>.

292 stars from the XSL library have BP/RP spectra, 302 stars from the UVES\_POP library, 381 stars from the NGSL library, and 255 from the STELIB library as listed in Table ???. By retaining stars non saturated, single, and by excluding peculiar stars confused or with emission lines, there remain 232 (XSL), 118 (UVES), and 198 (NGSL) stars, respectively. Furthermore, by considering only stars with average flux deviation between the high-resolution spectra and the BP/RP spectra within 1%, there remain 24 (XSL), 24 (UVES), 16 (NGSL), and 3 (STELIB) stars.

1sp

ì

## sectionReferences

- Bohlin, R. C., Deustua, S. E., & de Rosa, G. 2019, AJ, 158, 211
- Bohlin, R. C. & Lockwood, S. 2022, Update of the STIS CTE Correction Formula for Stellar Spectra, Instrument Science Report STIS 2022-7, 11 pages
- Borisov, S., Chilingarian, I., Rubtsov, E., et al. 2022, arXiv e-prints, arXiv:2211.09130
- Le Borgne, J. F., Bruzual, G., Pelló, R., et al. 2003, A&A, 402, 433
- Pal, T., Khan, I., Worthey, G., Gregg, M. D., & Silva, D. R. 2023, arXiv e-prints, arXiv:2301.05335
- Pancino, E., Sanna, N., Altavilla, G., et al. 2021, MNRAS, 503, 3660
- Verro, K., Trager, S. C., Peletier, R. F., et al. 2022, A&A, 660, A34

## 12 ACRONIMOUS

ACRONIMOUS listed to comment on the source (last column of the tables.cvs)

- SAT = satura o sospetta satura. Prevale su ogni altra flag
- VAR = classified as variable star by SIMBAD
- BIN = classified as binary star by SIMBAD
- WR = Wolf Rayet
- C = Carbon Star
- S = S stars (giants with ZrO bands)
- DMS = Double or multiple star
- YSO = Young Stellae Object
- Be = Be star
- BS = Blue Supergiant
- RSG = Red Supergiant
- EB = Eclipsing Binary
- ESG = Evolved Supergiant
- ELS = Emission Line Star
- ChP = Chemically Peculiar Star

=

PAGB = Post AGB star

HeAB = Herbig Ae/Be Star

BSS = Blue Straggler

CRO = lie in a very crowded field (ad judged from the DSS Simbad stamp image) - non indicato se già si applica un'altra flag

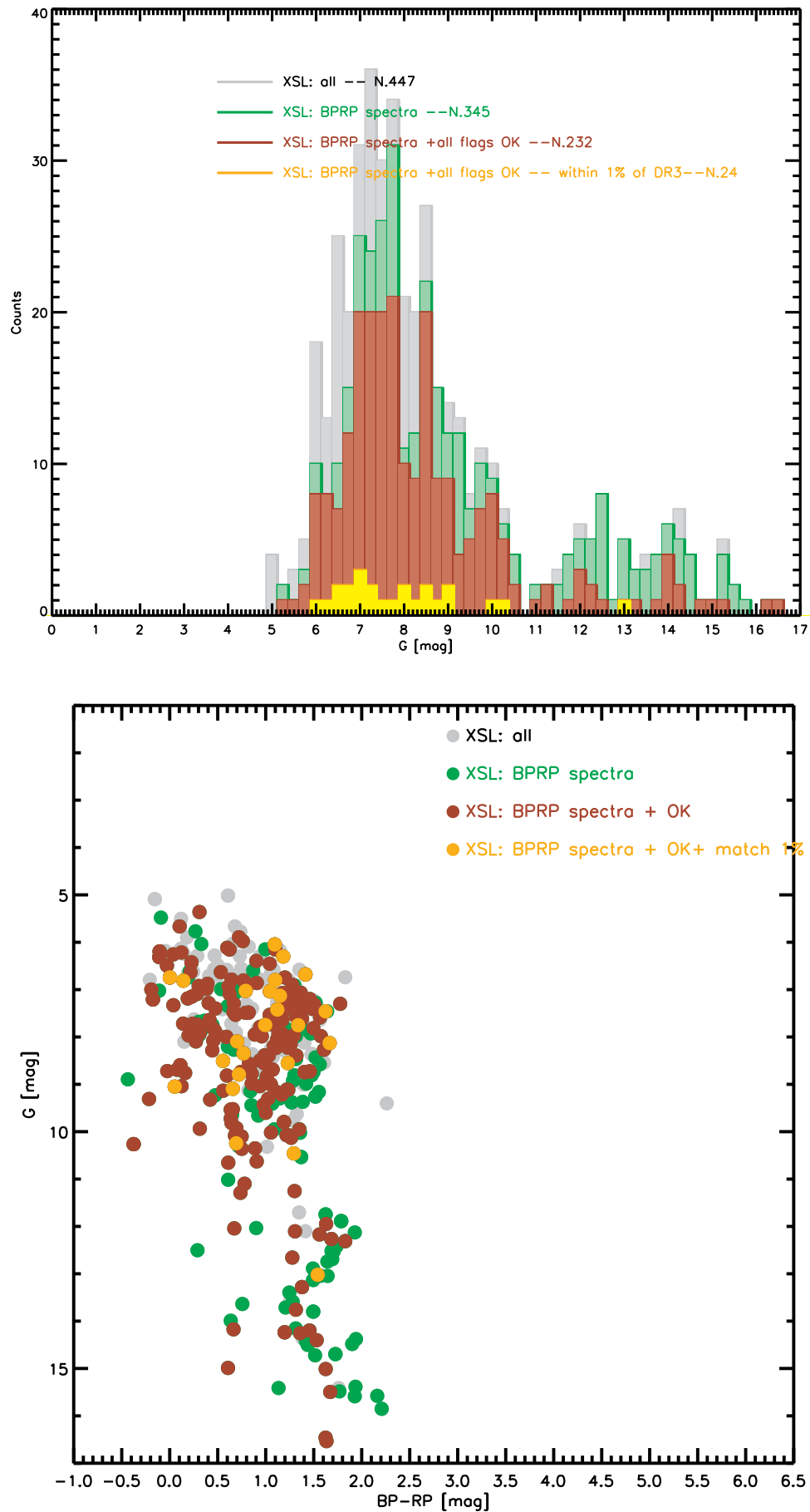


Fig. 43. Distributions of Gmag and BP/RP colors of the XSL matches with the BP/RP spectra.

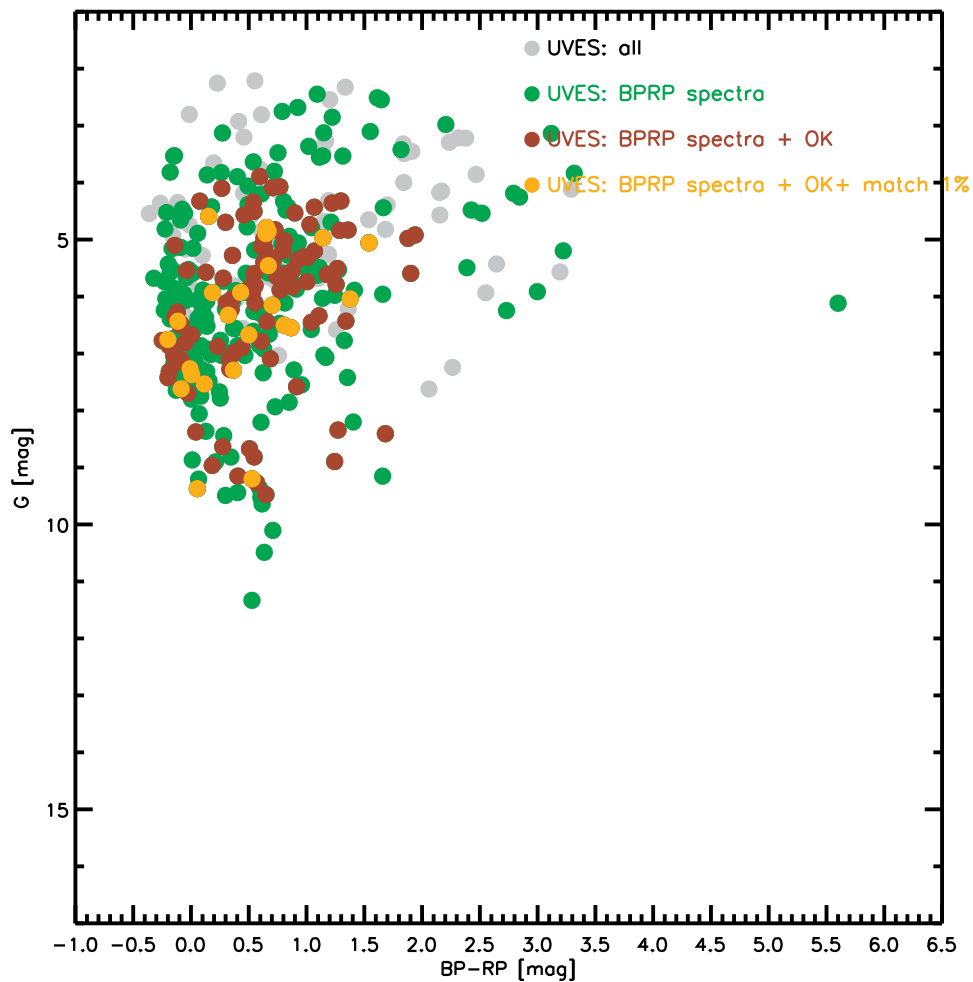
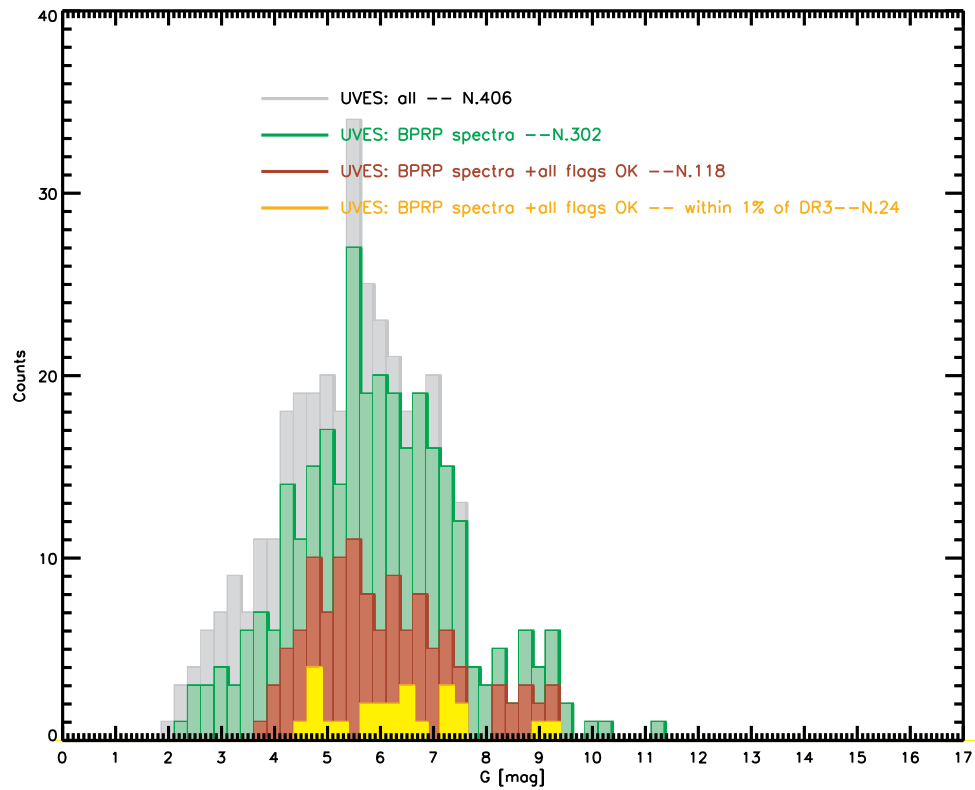


Fig. 44. Distributions of Gmag and BP/RP colors of the UVES\_POP matches with the BP/RP spectra.

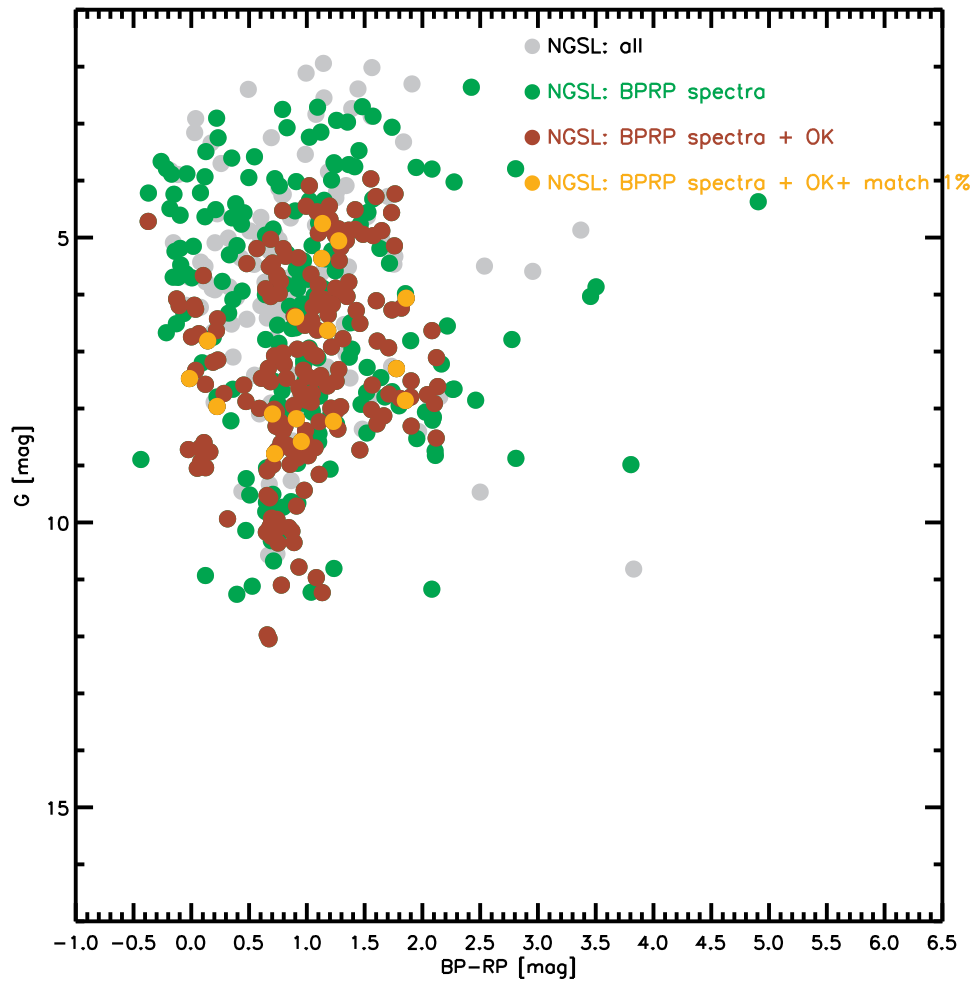
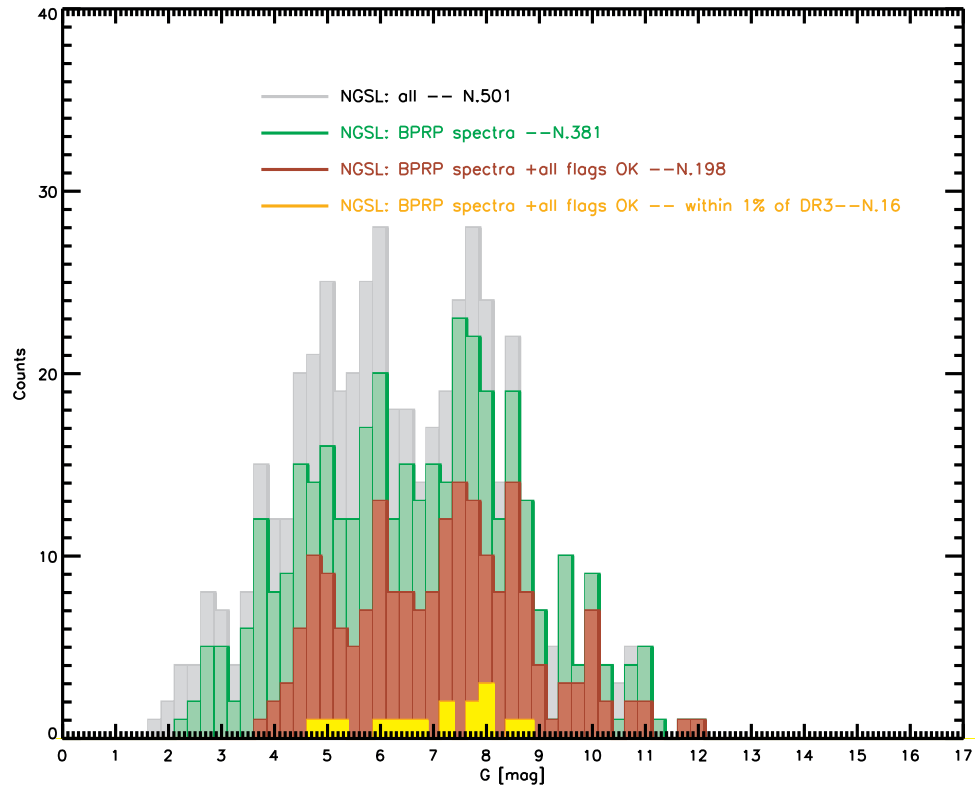


Fig. 45. Distributions of Gmag and BP/RP colors of the XSL matches with the BP/RP spectra.

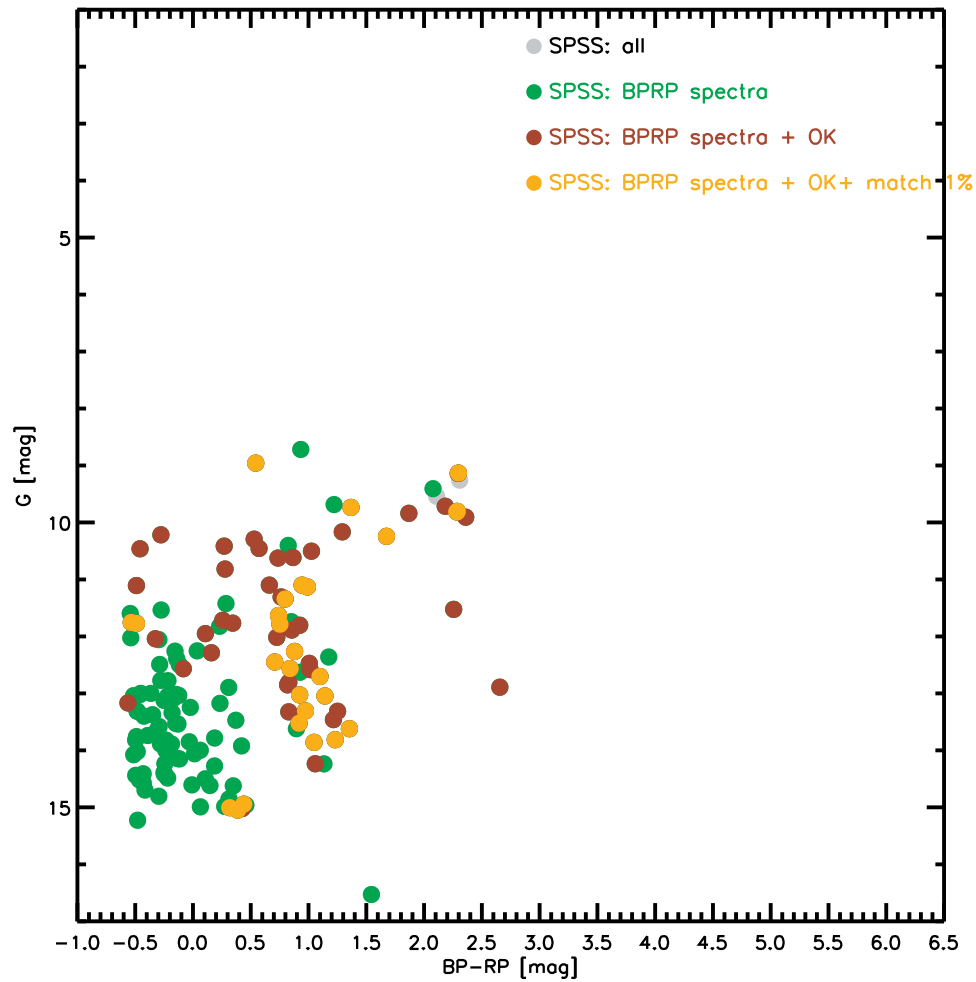
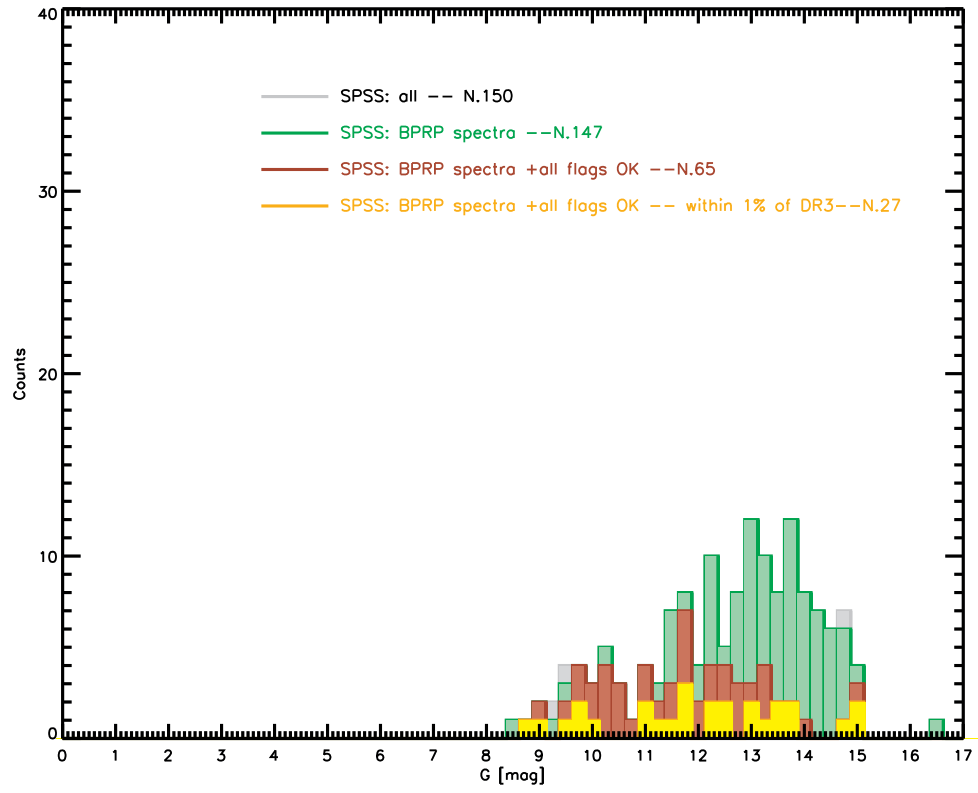
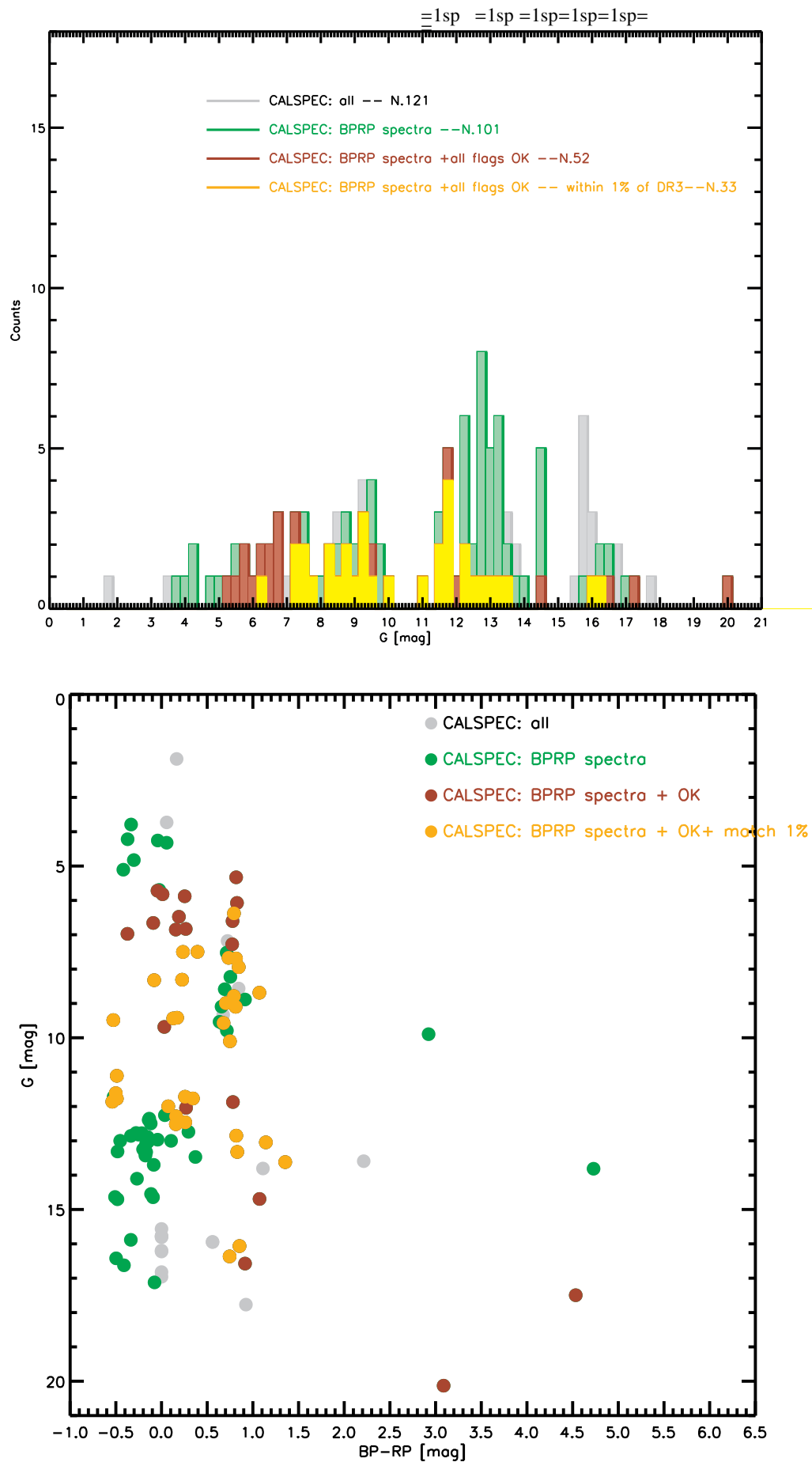


Fig. 46. Distributions of Gmag and BP/RP colors of the SPSS matches with the BP/RP spectra.



**Fig. 47.** Distributions of Gmag and BP/RP colors of the CALSPEC matches with the BP/RP spectra.